Uniparental nuclear inheritance following bisexual mating in fungi

Vikas Yadav, Sheng Sun, and Joseph Heitman*

Department of Molecular Genetics and Microbiology, Duke University Medical Center, Durham, NC 27710, USA

*Corresponding author

Joseph Heitman
Box 3546, 322 CARL Building, Research Drive
Department of Molecular Genetics and Microbiology
Duke University Medical Center
Durham, NC 27710
Phone: 919-684-2824
Fax: 919-684-2790
Email: heitm001@duke.edu

Running title: Pseudosexual reproduction in *Cryptococcus*

Keywords: Hybridogenesis; Meiosis; Nuclear migration, Dikaryotic fungi; Sexual parasitism, Pseudosexual reproduction.

Abstract

Some remarkable animal species require an opposite-sex partner for their sexual development but discard the partner's genome before gamete formation, generating hemi-clonal progeny in a process called hybridogenesis. Here, we discovered a similar phenomenon, termed pseudosexual reproduction, in a basidiomycete human fungal pathogen, *Cryptococcus neoformans*, where exclusive uniparental inheritance of nuclear genetic material was observed during bisexual reproduction. Analysis of strains expressing fluorescent reporter proteins revealed instances where only one of the parental nuclei was present in the terminal sporulating basidium. Whole-genome sequencing revealed the nuclear genome of the progeny was identical with one or the other parental genome. Pseudosexual reproduction was also detected in natural isolate crosses where it resulted in mainly *MAT*α progeny, a bias observed in *Cryptococcus* ecological distribution as well. The mitochondria in these progeny were inherited from the *MAT***a** parent, resulting in nuclear-mitochondrial genome exchange. The meiotic recombinase Dmc1 was found to be critical for pseudosexual reproduction. These findings reveal a novel, and potentially ecologically significant, mode of eukaryotic microbial reproduction that shares features with hybridogenesis in animals.

Introduction

Most multicellular organisms in nature undergo (bi)sexual reproduction involving two partners of the opposite sex to produce progeny. In most cases, following the fusion of the two haploid gametes, the diploid zygote receives one copy of the genetic material from each parent. To produce these haploid gametes, a diploid germ cell of the organism undergoes meiosis, which involves recombination between the two parental genomes, generating recombinant progeny. Recombination confers benefits by bringing together beneficial mutations and segregating away deleterious ones (Dimijian, 2005; Meirmans, 2009). In contrast, some organisms undergo variant forms of sexual reproduction, including parthenogenesis, gynogenesis, androgenesis, and hybridogenesis, and in doing so, produce clonal or hemi-clonal progeny (Avise, 2015; Neaves & Baumann, 2011).

In parthenogenesis, a female produces clonal progeny from its eggs without any contribution from a male partner (Avise, 2015; Hörandl, 2009). Gynogenesis and androgenesis occur when the fusion of an egg with a sperm induces cell division to produce clonal female or male zygotes, respectively (Lehtonen, Schmidt, Heubel, & Kokko, 2013). During hybridogenesis, an egg from one species fuses with the sperm from another species to generate a hybrid diploid zygote (Lavanchy & Schwander, 2019). However, one of the parental genomes is excluded during development, in a process termed genome exclusion that occurs before gametogenesis. The remaining parental genome undergoes replication followed by meiosis to produce an egg or a sperm. The sperm or egg then fuses with an opposite-sex gamete to generate a hemiclonal progeny. Because only one parent contributes genetic material to the progeny, but both parents are physically required, this phenomenon has been termed sexual parasitism (Lehtonen et al., 2013; Umphrey, 2006). While most of the reported cases of hybridogenesis are from female populations, recent reports suggest that it may also occur in male populations of some species (Dolezalkova et al., 2016; Schwander & Oldroyd, 2016). Currently, hybridogenesis has only been observed in the animal kingdom in some species of frogs, fishes, and snakes. Plants also exhibit parthenogenesis (aka apomixis), along with gynogenesis and androgenesis (Lehtonen et al., 2013; Mirzaghaderi & Horandl, 2016).

Unlike animals, most fungi do not have sex chromosomes; instead, cell-type identity is defined by the mating-type (*MAT*) locus (Heitman, 2015; Heitman, Sun, & James, 2013). While many fungi are heterothallic, with opposite mating-types in different individuals, and undergo

sexual reproduction involving two partners of compatible mating-types, other fungi are homothallic, with opposite mating-types residing within the same organism, and can undergo sexual production during solo culture in the absence of a mating partner. One class of homothallic fungi undergoes unisexual reproduction, during which cells of a single mating type undergo sexual reproduction to produce clonal progeny, similar to parthenogenesis (Heitman, 2015; Lee, Ni, Li, Shertz, & Heitman, 2010). Gynogenesis and hybridogenesis have not been identified in the fungal kingdom thus far.

Cryptococcus neoformans is a basidiomycete human fungal pathogen that exists as either one of two mating types, *MAT***a** or *MAT*α (Sun, Coelho, David-Palma, Priest, & Heitman, 2019). During sexual reproduction, two haploid yeast cells of opposite mating type interact and undergo cell-cell fusion (Kwon-Chung, 1975, 1976; Sun, Priest, & Heitman, 2019). The resulting dikaryotic zygote then undergoes a morphological transition and develops into hyphae whose termini mature to form basidia. In the basidium, the two parental nuclei fuse (karyogamy), and the resulting diploid nucleus undergoes meiosis to produce four daughter nuclei (Idnurm, 2010; Kwon-Chung, 1976; Sun, Priest, et al., 2019; Zhao, Lin, Fan, & Lin, 2019). These four haploid nuclei repeatedly divide via mitosis and bud from the surface of the basidium to produce four long spore chains. Interestingly, in addition to this canonical heterothallic sexual reproduction, a closely related species, *C. deneoformans* can undergo unisexual reproduction (Lin, Hull, & Heitman, 2005; Roth, Sun, Billmyre, Heitman, & Magwene, 2018; Sun, Billmyre, Mieczkowski, & Heitman, 2014).

In a previous study, we generated a genome-shuffled strain of *C. neoformans*, VYD135α, by using the CRISPR-Cas9 system targeting centromeric transposons in the lab strain H99α. This led to multiple centromere-mediated chromosome arm exchanges in strain VYD135α when compared to the parental strain H99α, without any detectable changes in gene content between the two genomes (Yadav, Sun, Coelho, & Heitman, 2020). Additionally, strain VYD135α exhibits severe sporulation defects when mated with strain KN99**a** (which is congenic with strain H99α but has the opposite mating type), likely due to the extensive chromosomal rearrangements introduced into the VYD135α strain. In this study, we show that the genome-shuffled strain VYD135α can in fact produce spores in crosses with *MAT***a** *C. neoformans* strains after prolonged incubation. Analysis of these spores reveals that the products from each individual basidium contain genetic material derived from only one of the two parents. Whole-

genome sequencing of the progeny revealed an absence of recombination between the two parental genomes. The mitochondria in these progeny were found to always be inherited from the *MAT***a** parent, consistent with known mitochondrial uniparental inheritance (UPI) patterns in *C. neoformans* (Sun, Fu, Ianiri, & Heitman, 2020). Using strains with differentially fluorescently labeled nuclei, we discovered that in a few hyphal branches as well as in basidia, only one of the two parental nuclei was present and produced spores, leading to uniparental nuclear inheritance. We also observed the occurrence of such uniparental nuclear inheritance in wild-type and natural isolate crosses. Furthermore, we found that the meiotic recombinase Dmc1 plays a central role during this unusual mode of reproduction of *C. neoformans*. Overall, this mode of sexual reproduction of *C. neoformans* exhibits striking parallels with hybridogenesis in animals.

Results

Chromosomal translocation strain exhibits unusual sexual reproduction

Previously, we generated a strain (VYD135α) with eight centromere-mediated chromosome translocations compared to the wild-type parental isolate H99α (Yadav et al., 2020). Co-incubation of the wild-type strain KN99**a** with the genome-shuffled strain VYD135α resulted in hyphal development and basidia production, but no spores were observed during a standard two-week incubation. However, when sporulation was assessed at later time points in the VYD135α x KN99**a** cross, we observed a limited number of sporulating basidia (16/1201=1.3%) after five weeks compared to a much greater level of sporulation in the wild-type H99α x KN99**a** cross (524/599 = 88%) (Figure 1A-D). None of these strains exhibited any filamentation on their own even after 5-weeks of incubation, indicating that the sporulation events were not a result of unisexual reproduction (Figure 1A-B). To analyze this delayed sporulation process in detail, spores from individual basidia were dissected and germinated to yield viable F1 progeny. As expected, genotyping of the mating-type locus in the H99α x KN99**a** progeny revealed the presence of both mating types in spores derived from each basidium (Figure 1E and G, Table 1). In contrast, the same analysis for VYD135α x KN99**a** revealed that all germinating progeny from each individual basidium possessed either only the *MAT*α or the *MAT***a** allele (Figure 1E and G, Table 1). PCR assays also revealed that the mitochondria in all of these progeny were inherited from the *MAT***a** parent, in accord with known UPI (Figure 1F-G).

These results suggest the inheritance of only one of the parental nuclei in the VYD135α x KN99**a** F1 progeny. The presence of mitochondria from only the *MAT***a** parent in *MAT*α progeny further confirmed that these progeny were the products of fusion between the parent strains and were not the products of unisexual reproduction.

Fluorescence microscopy reveals uniparental nuclear inheritance after mating

Next, we tested whether the uniparental inheritance detected at the *MAT* locus also applied to the entire nuclear genome. To address this, we established a fluorescence-based assay in which the nuclei of strains H99α and VYD135α were labeled with GFP-H4, whereas the KN99**a** nucleus was marked with mCherry-H4. In a wild-type cross (H99α x KN99**a**), the nuclei in the hyphae as well as in the spores were yellow to orange because both nuclei were in a common cytoplasm and thus incorporated both the GFP- and the mCherry-tagged histone H4 proteins (Figure 2-figure supplement 1A and B). We hypothesized that in the cases of uniparental nuclear inheritance, only one of the nuclei would reach the terminal basidium and would thus harbor only one fluorescent nuclear color signal (Figure 2-figure supplement 1A).

After establishing this fluorescent tagging system using the wild-type strains H99α x KN99**a**, shuffled-strain VYD135α x KN99**a** crosses with fluorescently labeled strains were examined. In the wild-type cross, most of the basidia formed robust spore chains with both fluorescent colors observed in them, while a small population (~1%) of basidia exhibited spore chains with only one color, representing uniparental nuclear inheritance (Figure 2A and Figure 2-figure supplement 2A). In contrast, the majority of the basidium population in the shuffled-strain VYD135α x KN99**a** cross did not exhibit sporulation, and the two parental nuclei appeared fused but undivided (Figure 2B and Figure 2-figure supplement 2B). A few basidia (~1%) bore spore chains with only one fluorescent color, marking uniparental nuclear inheritance events. While the basidia with uniparental nuclear inheritance in the H99α x KN99**a** cross were a small fraction (~1%) of sporulating basidia, the uniparental basidia accounted for all of the sporulating basidia in the VYD135α x KN99**a** cross. Taken together, these results show that the uniparental nuclear inheritance leads to the generation of clonal progeny but requires mating, cell-cell fusion between parents of two opposite mating types. Thus, this process defies the main purpose of sexual reproduction, which is to produce recombinant progeny from two parents. Based on these observations, we define the process of uniparental nuclear inheritance during sporulation in *C.*

neoformans as pseudosexual reproduction (and it is referred to as such hereafter). The progeny obtained via this process will be referred to as the uniparental progeny because they inherit a nuclear genome derived from only one of the two parents.

Pseudosexual reproduction also occurs in natural isolates

After establishing the pseudosexual reproduction of lab strains, we sought to determine whether such events also occur with natural isolates. For this purpose, we selected two wild-type natural isolates, Bt63**a** and IUM96-2828**a** (referred to as IUM96**a** hereafter) (Desjardins et al., 2017; Keller, Viviani, Esposto, Cogliati, & Wickes, 2003; Litvintseva et al., 2003). IUM96**a** belongs to the same lineage as H99α/KN99**a** (VNI) and exhibits approximately 0.1% genome divergence from the H99α reference genome. Bt63**a** belongs to a different lineage of the *C. neoformans* species (VNBI) and exhibits ~0.5% genetic divergence from the H99α/KN99**a** genome. Both the Bt63**a** and the IUM96**a** genomes exhibit one reciprocal chromosome translocation with H99α, and as a result, share a total of ten chromosome-level changes with the genome-shuffled strain VYD135α (Figure 3A). None of these strains are self-filamentous even after prolonged incubation on mating media but both cross efficiently with H99α and VYD135α (Figure 3-figure supplement 1A).

The H99α x Bt63**a** strains crossed rapidly (within a week) producing robust sporulation from most of the basidia observed. The VYD135α x Bt63**a** cross underwent a low frequency of sporulation (12 spore-producing basidia/840 basidia=1.4%) in 2 to 3 weeks (Figure 3-figure supplement 1B). Dissection of spores from the H99α x Bt63**a** cross revealed a low germination frequency (average of 25%) with two of the basidia showing no spore germination at all (Supplementary file 1a). This result is consistent with previous results, and the low germination frequency could be explained by the genetic divergence between the two strains (Morrow et al., 2012). Genotyping of germinated spores from the H99α x Bt63**a** cross revealed both *MAT***a** and *MAT*α progeny from individual basidia, with almost 75% of the meiotic events generating progeny that were heterozygous for the *MAT* locus (Figure 3-figure supplement 1C and Supplementary file 1a). For the VYD135α x Bt63**a** cross, spores from 15/20 basidia germinated and displayed a higher germination frequency than the H99α x Bt63**a** cross (Supplementary file 1a). Interestingly, all germinated progeny harbored only the *MAT*α mating-type, whereas the

mitochondria were in all cases inherited from the *MAT***a** parent (Figure 3-figure supplement 1C). These results suggest that pseudosexual reproduction also occurs with Bt63**a** and accounts for the high germination frequency of progeny from the VYD135α x Bt63**a** cross. The occurrence of pseudosexual reproduction was also identified using the fluorescence-based assay with crosses between the GFP-H4 tagged VDY135α and mCherry-H4 tagged Bt63**a** strains (Figure 3-figure supplement 2).

Crosses with strain IUM96**a** also revealed a low level of sporulation (19/842=2.3%) with VYD135α but a high sporulation frequency with H99α (91%) (Figure 3-figure supplement 1D). Analysis of progeny from crosses involving IUM96**a** revealed a similar pattern to what was observed with crosses involving KN99**a**. The progeny from H99α x IUM96**a** exhibited variable basidium-specific germination frequencies and inherited both *MAT***a** and *MAT*α in each basidium, whereas VYD135α x IUM96**a** progeny from each basidium inherited exclusively either *MAT***a** or *MAT*α (Figure 3-figure supplement 1E, and Supplementary file 1b). Interestingly, we observed co-incident uniparental *MAT* inheritance and a high germination frequency in progeny of basidia 7, 8, and 9 from the H99α x IUM96**a** cross as well (Figure 3-figure supplement 1E, and Supplementary file 1b). Taken together, these results suggest that this unusual mode of sexual reproduction occurs with multiple natural isolates. We further propose that pseudosexual reproduction occurs in nature in parallel with canonical sexual reproduction.

Uniparental progeny completely lack signs of nuclear recombination between the two parents

As mentioned previously, H99α (as well as the H99α-derived strain VYD135α) and Bt63**a** have approximately 0.5% genetic divergence. The occurrence of pseudosexual reproduction in the VYD135α x Bt63**a** cross allowed us to test if the two parental genomes recombine with each other during development. We subjected progeny from crosses VYD135α x Bt63**a** and H99α x Bt63**a** to whole-genome sequencing. As expected, for the H99α x Bt63**a** cross, both parents contributed to the nuclear composition of their progeny, and there was clear evidence of meiotic recombination as determined by variant analysis (Figure 3B). However, when the VYD135α x Bt63**a** progeny were similarly analyzed, the nuclear genome in each of the progeny was found to be inherited exclusively from only the VYD135α parent (Figure 3C and

Figure 3-figure supplement 3), and the progeny exhibited sequence differences across the entire Bt63**a** genome. In contrast, the mitochondrial genome was inherited exclusively from the Bt63**a** parent (Figure 3D and Figure 3-figure supplement 4), in accord with the PCR assay results discussed above. Additionally, the whole-genome sequencing data also revealed that while most of the H99α x Bt63**a** progeny exhibited aneuploidy, the genome-shuffled strain VYD135α x Bt63**a** progeny were euploid (Figure 3-figure supplement 5A and B), and based on flow cytometry analysis, these uniparental progeny were haploid (Figure 3-figure supplement 5C).

The progeny from crosses involving IUM96**a** as the *MAT***a** partner were also sequenced. Similar to the Bt63**a** analysis, the H99α x IUM96**a** progeny exhibited signs of meiotic recombination, whereas the VYD135α x IUM96**a** progeny did not (Figure 3-figure supplement 6). Congruent with the mating-type analysis, the progeny in each of the basidia exclusively inherited nuclear genetic material from only one of the two parents. Furthermore, the H99α x IUM96**a** progeny were found to be aneuploid for some chromosomes, while the progeny of VYD135α x IUM96**a** were completely euploid (Figure 3-figure supplement 7). We also sequenced four progeny from basidium 7 from the H99α x IUM96**a** cross, which were suspected to be uniparental progeny based on mating-type PCRs. This analysis showed that all four progeny harbored only H99α nuclear DNA and had no contribution from the IUM96**a** nuclear genome, further supporting the conclusion that pseudosexual reproduction occurs in wild-type crosses (Figure 3-figure supplement 6A). Similar to other progeny, the mitochondria in these progeny were inherited from the *MAT***a** parent (Figure 3-figure supplement 1E, and Supplementary file 1b). Combined, these results affirm the occurrence of a novel mode of sexual reproduction in *C. neoformans*, which is initiated by the fusion of two strains of opposite mating types, but whose progeny inherit DNA exclusively from one parent.

Pseudosexual reproduction stems from nuclear loss via hyphal branches

Fluorescence microscopy revealed that only one of the two parental nuclei undergoes meiosis and produces spores in approximately 1% of the total basidia population. Based on this finding, we hypothesized that the basidia with only one parental nucleus might arise due to nuclear segregation events during hyphal branching. To gain further insight into this process, the nuclear distribution pattern along the sporulating hyphae was studied. As expected, imaging of long hyphae in the wild-type cross revealed the presence of pairs of nuclei with both fluorescent

markers along the length of the majority of hyphae (Figure 4A). In contrast, tracking of hyphae from basidia with spore chains in the genome-shuffled strain VYD135α x KN99**a** cross revealed hyphal branches with only one parental nucleus, which were preceded by a hyphum with both parental nuclei (Figure 4B, Figure 4-figure supplement 1A and B). Unfortunately, a majority of the hyphae (>30 independent hyphae) we tracked were embedded into the agar, and most of these could not be tracked to the point of branching. For some others, we were able to image the hyphal branching point where two nuclei separate from each other but were then either broken or did not have mature basidia on them (Figure 4-figure supplement 1B). In total, we observed seven events of nuclear loss at hyphal branching in independent experiments and were able to track two of them to observe sporulation or basidia formation at the tip. We also observed long hyphae with only one parental nucleus in the VYD135α x Bt63**a** cross as well, suggesting the mechanism might be similar between strains.

These results suggest that hyphal branching may facilitate the separation of one parental nucleus from the main hyphae harboring both parental nuclei. While this is the most plausible explanation based on our results, we cannot rule out other possible mechanisms, such as a role for clamp cells, leading to nuclear separation during hyphal growth. As a result, one of the parental genomes is excluded at a step before diploidization and meiosis, similar to the process of genome exclusion observed in hybridogenesis. We hypothesize that nuclear segregation can be followed by endoreplication occurring in these hyphal branches or in the basidium to produce a diploid nucleus that then ultimately undergoes meiosis and produces uniparental progeny, which will be explored in future studies.

Meiotic recombinase Dmc1 is important for pseudosexual reproduction

Because the genomes of the uniparental progeny did not show evidence of meiotic recombination between the two parents, we tested whether pseudosexual reproduction involves meiosis. Additionally, we sought to test our hypothesis that pseudosexual reproduction involves endoreplication that is followed by meiosis. We therefore tested whether Dmc1, a key component of the meiotic machinery, is required for pseudosexual reproduction. The meiotic recombinase gene *DMC1* was deleted in congenic strains H99α, VYD135α, and KN99**a**, and the resulting mutants were subjected to crossing. A previous report documented that *dmc1*Δ bilateral crosses (both the parents are mutant for *DMC1*) display significantly reduced, but not completely

abolished, sporulation in *Cryptococcus* (Lin et al., 2005). We observed a similar phenotype with the H99α *dmc1*Δ x KN99**a** *dmc1*Δ cross. While most of the basidia were devoid of spore chains, a small percentage (21/760=2.7%) of the population bypassed the requirement for Dmc1 and produced spores (Figure 5A and Figure 5-figure supplement 1A). When dissected, the germination frequency for these spores was found to be very low (~22% on average) with spores from many basidia not germinating at all (Supplementary File 1c). Furthermore, *MAT*-specific PCRs revealed that some of the progeny were aneuploid or diploid. For VYD135α *dmc1*Δ x KN99**a** *dmc1*Δ, many fewer basidia (~0.1%) produced spore chains as compared to ~1% sporulation in VYD135α x KN99**a** (Figure 5A, B and Figure 5-figure supplement 1B). *dmc1* mutant unilateral crosses (one of the two parents is mutant and the other one is wild-type) sporulated at a frequency of 0.4% suggesting that only one of the parental strains was producing spores (Figure 5B). When a few sporulating basidia from the VYD135α *dmc1*Δ x KN99**a** *dmc1*Δ bilateral cross were dissected, two different populations of basidia emerged, one with no spore germination, and the other with a high spore germination frequency and uniparental *MAT* inheritance (Supplementary File 1c). We hypothesize that the basidia with a high spore germination frequency represent those that have escaped the normal requirement for Dmc1. Overall, the *DMC1* deletion led to a 20-fold reduction in viable sporulation in the VYD135α x KN99**a** cross, observed as a 10-fold decrease from the number of sporulation events in the bilateral cross and a further 2-fold reduction in the number of basidia producing viable spores.

To further support these findings, *DMC1* was deleted in mCherry-H4 tagged KN99**a** and crossed with GFP-H4 tagged VYD135α. We hypothesized that GFP-H4 tagged VYD135α would produce spore chains in this cross because it harbors *DMC1*, whereas mCherry-H4 tagged KN99**a** *dmc1*Δ would fail to do so. Indeed, all 11 observed basidia with only the GFP-H4 fluorescence signal were found to produce spores, but only 2 out of 19 mCherry-H4 containing basidia exhibited sporulation (Figure 5-figure supplement 2). These results combined with the spore dissection findings show that Dmc1 is critical for pseudosexual reproduction. While these results provide concrete evidence for meiosis as a part of pseudosexual reproduction, they also suggest the occurrence of a preceding endoreplication event. However, further studies will need to be conducted to validate and confirm endoreplication or alternate mechanisms to achieve the ploidy necessary for a classical meiosis event.

Discussion

Hybridogenesis and parthenogenesis are mechanisms that allow some organisms to overcome some hurdles of sexual reproduction and produce hemiclonal or clonal progeny (Avise, 2015; Hörandl, 2009; Lavanchy & Schwander, 2019). However, harmful mutations are not filtered in these processes, making them disadvantageous during evolution and thus restricting the occurrence of these processes to a limited number of animal species (Lavanchy & Schwander, 2019). In this study, we discovered and characterized the occurrence of a phenomenon in fungi that resembles hybridogenesis and termed it pseudosexual reproduction (Figure 6- figure supplement 1). Fungi are known to exhibit asexual, (bi)sexual, unisexual, and parasexual reproduction and can switch between these reproductive modes depending on environmental conditions (Heitman, 2015; Heitman et al., 2013). The discovery of pseudosexual reproduction further diversifies known reproductive modes in fungi, suggesting the presence of sexual parasitism in this kingdom.

Hybridogenesis in animals occurs between two different species. The result of hybridogenesis is the production of gametes that are clones of one of the parents, which then fuse with an opposite-sex gamete of the second species, generating hemiclonal offspring. In our study, we observed a similar phenomenon where only one parent contributes to spores, the counterpart of mammalian gametes. However, we observed this phenomenon occurring between different strains of the same species, *C. neoformans*. It is important to note that these strains vary significantly from each other in terms of genetic divergence and in one case by chromosome rearrangements to the extent that they could be considered different species. This suggests that hybridogenesis in animals and pseudosexual reproduction in fungi are similar to each other. Hybridogenesis requires the exclusion of one of the parents, which is followed by endoreplication of the other parent's genome and meiosis. The whole-genome sequence of the progeny in our study revealed the complete absence of one parent's genome, suggesting manifestations of genome exclusion during hyphal growth. The mechanism by which the retained parental genome increases its ploidy before meiosis remains to be further investigated in *C. neoformans*. Endoreplication is known to occur in the sister species *C. deneoformans* during unisexual reproduction, and we think that this is the most likely route via which ploidy is increased during pseudosexual reproduction.

The mechanism and time of genome exclusion during hybridogenesis in animals are not entirely understood, except for a few insights from triploid fishes of the genus *Poeciliopsis* and water frogs, *Pelophylax esculentus*. Studies using *Poeciliopsis* fishes showed that haploid paternal genome exclusion takes place during the onset of meiosis via the formation of a unipolar spindle, and thus, only the diploid set of maternal chromosomes is retained (Cimino, 1972a, 1972b). On the other hand, studies involving *P. esculentus* revealed that genome exclusion occurs during mitotic division, before meiosis, which is followed by endoreplication of the other parental genome (Heppich, Tunner, & Greilhuber, 1982; Tunner & Heppich-Tunner, 1991; Tunner & Heppich, 1981). A recent study, however, proposed that genome exclusion in *P. esculentus* could also take place during early meiotic phases (Dolezalkova et al., 2016). Using fluorescence microscopy, we examined the steps of nuclear exclusion in *C. neoformans* and found that it occurs during mitotic hyphal growth and not during meiosis. We also observed that genome exclusion could happen with either of the two parents in *C. neoformans*, similar to what has also been reported for water frogs. However, for most other species, genome exclusion was found to occur with the male genome only, leaving behind the female genome for meiosis (Cimino, 1972a; Holsbeek & Jooris, 2009; Lavanchy & Schwander, 2019; Umphrey, 2006; Uzzell, Günther, & Berger, 1976; Vinogradov, Borkin, Gunther, & Rosanov, 1991). Multiple studies have shown the formation of meiotic synaptonemal complexes during hybridogenesis, clearly establishing the presence of meiosis during this process (Dedukh et al., 2019; Dedukh et al., 2020; Nabais, Pereira, Cunado, & Collares-Pereira, 2012). Our results showed that the meiotic recombinase Dmc1 is required for pseudosexual reproduction, suggesting the presence of meiosis, whereas there is no direct evidence for the role of a meiotic recombinase in hybridogenetic animals. Taken together, these results indicate that the mechanism might be at least partially conserved across distantly related species. Future studies will shed more light on this, and if established, the amenability of *C. neoformans* to genetic manipulation will aid in deciphering some of the unanswered questions related to hybridogenesis in animals.

The occurrence of pseudosexual reproduction might also have significant implications for *C. neoformans* biology. Most (>95%) of *Cryptococcus* natural isolates belong to only one mating type, α (Zhao et al., 2019). While the reason behind this distribution is unknown, one explanation could be the presence of unisexual reproduction in the sister species *C. deneoformans* and *C. gattii* (Fraser et al., 2005; Lin et al., 2005; Phadke, Feretzaki, Clancey,

Mueller, & Heitman, 2014). The presence of pseudosexual reproduction in *C. neoformans* might help explain the mating-type distribution pattern for this species. In this report, one of the *MAT***a** natural isolates, Bt63**a**, did not contribute to pseudosexual reproduction and the other isolate, IUM96**a**, produced uniparental progeny in only one basidium, while the rest of the basidia produced *MAT*α progeny. We hypothesize that *MAT***a** isolates may be defective in this process due to either a variation in their genomes or some other as yet undefined sporulation factor. As a result, pseudosexual reproduction could lead to the generation of predominantly α progeny in nature, reducing the *MAT***a** population and thus favoring the expansion of the α mating-type population. However, it is still possible that the preferential inheritance of the nuclear genome from one of the two parents is decided by genetic elements located in regions other than *MAT*, and whether the uniparental nuclear inheritance is mating-type specific remains to be elucidated. Furthermore, the occurrence of pseudosexual reproduction in other pathogenic species such as *C. deneoformans* and non-pathogenic species such as *C. amylolentus* will be investigated in future studies. Attempts to identify the occurrence of pseudosexual reproduction between species where hybrids are known to occur, *C. neoformans* and *C. deneoformans* hybrids, will also be made. These studies will help establish the scope of pseudosexual reproduction in *Cryptococcus* species and could be extended to other basidiomycetes.

We propose that pseudosexual reproduction can occur between any two opposite mating-type strains as long as each of them is capable of undergoing cell-cell fusion and at least one of them can sporulate. We speculate that pseudosexual reproduction might play a key role in *C. neoformans* survival during unfavorable conditions. In conditions where two mating partners are fully compatible, pseudosexual reproduction will be mostly hidden and might not be important (Figure 6, top panel). However, when the two mating partners are partially incompatible or completely incompatible due to high genetic divergence or karyotypic variation, pseudosexual reproduction will be important (Figure 6, left, right, and bottom panels). For example, most of the basidia in H99α and Bt63**a** cross largely produce aneuploid and/or inviable progeny leading to unsuccessful sexual reproduction. However, a small yet significant proportion of the basidia generate clonal yet viable and fit progeny via pseudosexual reproduction. We hypothesize that these progeny will have a better chance of survival and find a suitable mating partner in the environment whereas, the unfit recombinant progeny might fail to do so. In nature, this might allow a new genotype/karyotype to not only survive but also expand and will prove

advantageous. If a new genotype/karyotype had only the option of undergoing sexual reproduction, it might not survive, restricting the evolution of a new strain. Overall, this mode of pseudosexual reproduction might act as an escape path from genomic incompatibilities between two related isolates and allow them to produce spores for dispersal.

One of the key differences between pseudosexual reproduction and unisexual reproduction observed in the *Cryptococcus* species complex is the inheritance of mitochondrial DNA. While both unisexual and pseudosexual reproduction result in clonal progeny with respect to the nuclear genome, the mitochondria in pseudosexual reproduction are almost exclusively inherited from the *MAT***a** parent (Figure 6- figure supplement 1). This results in the exchange of mitochondrial DNA in the progeny that inherit the *MAT*α nuclear genome, resembling the nuclear-mitochondrial exchange observed during cytoduction in *Saccharomyces cerevisiae*. During cytoduction, mutants defective in nuclear fusion produce haploid progeny with nuclear genome from one parent, but a mixture of both parents cytoplasm resulting in the inheritance of one parental mitochondrial genome with the other parent's nuclear genome (Conde & Fink, 1976; Lancashire & Mattoon, 1979; Zakharov & Yarovoy, 1977). This process was used to study mitochondrial genetics with respect to the transfer of drug-resistance genes and other mitochondrial mutations. Similar to cytoduction, pseudosexual reproduction could be employed to study mitochondrial genetics, such as functional analysis of mitochondrial encoded drug resistance, and cytoplasmic inheritance of factors such as prions in *C. neoformans*.

The fungal kingdom is one of the more diverse kingdoms with approximately 3 million species (Sun, Hoy, & Heitman, 2020). The finding of hybridogenesis-like pseudosexual reproduction hints towards unexplored biology in this kingdom that might provide crucial clues for understanding the evolution of sex. Fungi have also been the basis of studies focused on understanding the evolution of meiosis, and the presence of genome reduction, as well as the parasexual cycle in fungi, have led to the proposal that meiosis evolved from mitosis (Hurst & Nurse, 1991; Wilkins & Holliday, 2009). Pseudosexual reproduction may be a part of an evolutionary process wherein genome exclusion followed by endoreplication and meiosis was an ancestral form of reproduction that preceded the evolution of sexual reproduction. Evidence supporting such a hypothesis can be observed in organisms undergoing facultative sex or facultative parthenogenesis (Booth et al., 2012; Fields, Feldheim, Poulakis, & Chapman, 2015; Hodač, Klatt, Hojsgaard, Sharbel, & Hörandl, 2019; Hojsgaard & Harandl, 2015). The presence

of these organisms also suggests that a combination of both sexual and clonal modes of reproduction might prove to be evolutionarily advantageous.

Materials and Methods

Strains and media

C. neoformans wild-type strains H99α and KN99**a** served as the wild-type isogenic parental lineages for the experiments (Nielsen et al., 2003; Perfect, Ketabchi, Cox, Ingram, & Beiser, 1993), in addition to *MAT***a** strains Bt63**a** and IUM96-2828**a** (Keller et al., 2003; Litvintseva et al., 2003). Strains were grown in YPD media for all experiments at 30°C unless stated otherwise. G418 and/or NAT were added at a final concentration of 200 and 100 µg/ml, respectively, for the selection of transformants. MS media was used for all the mating assays, which were performed as described previously (Sun, Priest, et al., 2019). Basidia-specific spore dissections were performed after two-five weeks of mating, and the spore germination frequency was scored after five days of dissection. All strains and primers used in this study are listed in Supplementary File 1d and Supplementary File 1e, respectively.

Genotyping for mating-type locus and mitochondria

Mating-type (*MAT*) and mitochondrial genotyping for all the progeny were conducted using PCR assays. Genomic DNA was prepared using the MasterPure^{TM} Yeast DNA purification kit from Lucigen. To determine the *MAT,* the *STE20* allele present within the *MAT* locus was detected because it differs in length between the two different mating types. Primers specific to both *MAT***a** and *MAT*α (JOHE50979-50982 in Supplementary File 1e) were mixed in the same PCR mix, and the identification was made based on the length of the amplicon (Figure 1E-G). For the mitochondrial genotyping, the *COX1* allele present in the mitochondrial DNA was probed to distinguish between H99α/VYD135α and KN99**a**/IUM96**a**. For the differentiation between Bt63**a** and H99α/VYD135α, the *COB1* allele was used because *COX1* in Bt63**a** is identical to H99α/VYD135α. The difference for both *COX1* and *COB1* is the presence or absence of an intron and results in significantly different size products between *MAT*α and *MAT***a** parents (Figure 1 and Figure 3-figure supplement 1). The primers used for these assays (JOHE51004-51007) are mentioned in Supplementary File 1e.

Genomic DNA isolation for sequencing

Genomic DNA for whole-genome sequencing was prepared using the CTAB-based lysis method, as described previously (Yadav et al., 2020). Briefly, 50 ml of an overnight culture was pelleted, frozen at -80°C, and subjected to lyophilization. The lyophilized cell pellet was broken into a fine powder, mixed with lysis buffer, and the mix was incubated at 65°C for an hour with

intermittent shaking. The mix was then cooled on ice, and the supernatant was transferred into a fresh tube, and an equal volume of chloroform (~15 ml) was added and mixed. The mix was centrifuged at 3200 rpm for 10 min, and the supernatant was transferred to a fresh tube. An equal volume of isopropanol (~18 to 20 ml) was added into the supernatant and mixed gently. This mix was incubated at -20°C for an hour and centrifuged at 3200 rpm for 10 min. The supernatant was discarded, and the DNA pellet was washed with 70% ethanol. The pellet was air-dried and dissolved in 1ml of RNase containing 1X TE buffer and incubated at 37°C for 45 min. The DNA was again chloroform purified and precipitated using isopropanol, followed by ethanol washing, air drying, and finally dissolved in 200 µl 1X TE buffer. The DNA quality was estimated with NanoDrop, whereas DNA quantity was estimated with Qubit.

Whole-genome Illumina sequencing, ploidy, and SNP analysis

Illumina sequencing of the strains was performed at the Duke sequencing facility core (https://genome.duke.edu/), using Novaseq 6000 as 150 paired-end sequencing. The Illumina reads, thus obtained, were mapped to the respective genome assembly (H99, VYD135, Bt63, or IUM96) using Geneious (RRID:SCR_010519) default mapper to estimate ploidy. The resulting BAM file was converted to a .tdf file, which was then visualized through IGV to estimate the ploidy based on read coverage for each chromosome.

For SNP calling and score for recombination in the progeny, Illumina sequencing data for each progeny was mapped to parental strain genome assemblies individually using the Geneious default mapper with three iterations. The mapped BAM files were used to perform variant calling using Geneious with 0.8 variant frequency parameter and at least 90x coverage for each variant. The variants thus called were exported as VCF files and imported into IGV for visualization purposes. H99, Bt63, IUM96-2828, and VYD135 Illumina reads were used as controls for SNP calling analysis.

PacBio/Nanopore genome assembly and synteny comparison

To obtain high-molecular-weight DNA for Bt63 genome PacBio and IUM96-2828 genome Nanopore sequencing, DNA was prepared as described above. The size estimation of DNA was carried out by electrophoresis of DNA samples using PFGE. For this purpose, the PFGE was carried out at 6V/cm at a switching frequency of 1 to 6 sec for 16 h at 14°C. Samples with most of the DNA ≥100 kb or larger were selected for sequencing. For PacBio sequencing, the DNA sample was submitted to the Duke sequencing facility core. Nanopore sequencing was

515 performed in our lab using a MinION device on an R9.4.1 flow cell. After sequencing, reads
516 were assembled to obtain a Bt63 genome assembly via Canu (RRID:SCR_015880) using PacBio
517 reads > 2 kb followed by five rounds of pilon polishing (RRID:SCR_014731). For IUM96-2828,
518 one round of nanopolish was also performed before pilon polishing. Once completed, the
519 chromosomes were numbered based on their synteny with the H99 genome. For chromosomes
520 involved in translocation (Chr 3 and Chr 11), the chromosome numbering was defined by the
521 presence of the respective syntenic centromere from H99. Centromere locations were mapped
522 based on BLASTn analysis with H99 centromere flanking genes.
523 Synteny comparisons between the genomes were performed with SyMAP v4.2 using
524 default parameters (Soderlund, Bomhoff, & Nelson, 2011)
525 (http://www.agcol.arizona.edu/software/symap/). The comparison block maps were exported as
526 .svg files and were then processed using Adobe® Illustrator® (RRID:SCR_010279) and Adobe®
527 Photoshop® (RRID:SCR_014199) for representation purposes. The H99 genome was used as the
528 reference for comparison purposes for plotting VYD135, Bt63, and IUM96-2828 genomes. The
529 centromere and telomere locations were manually added during the figure processing.
530 ***Fluorescent tagging and microscopy***
531 GFP and mCherry tagging of histone H4 were performed by integrating respective
532 constructs at the safe haven locus (Arras, Chitty, Blake, Schulz, & Fraser, 2015). GFP-H4
533 tagging was done using the previously described construct, pVY3 (Yadav & Sanyal, 2018). For
534 mCherry-H4 tagging, the GFP-containing fragment in pVY3 was excised using SacI and BamHI
535 and was replaced with mCherry sequence PCR amplified from the plasmid pLKB25
536 (Kozubowski & Heitman, 2010). The constructs were then linearized using XmnI and
537 transformed into desired strains using CRISPR transformation, as described previously (Fan &
538 Lin, 2018). The transformants were screened by PCR, and correct integrants were obtained and
539 verified using fluorescent microscopy.
540 To observe the fluorescence signals in the hyphae and basidia, a 2-3 week old mating
541 patch was cut out of the plate and directly inverted onto a coverslip in a glass-bottom dish. The
542 dish was then used to observe filaments under a DeltaVision microscope available at the Duke
543 University Light Microscopy Core Facility (https://microscopy.duke.edu/dv). The images were
544 captured at 60X magnification with 2x2 bin size and z-sections of either 1 or 0.4 µm each. GFP
545 and mCherry signals were captured using the GFP and mCherry filters in the Live-Cell filter set.

The images were processed using Fiji-ImageJ (https://imagej.net/Fiji) (RRID:SCR_002285) and exported as tiff files as individual maximum projected images. The final figure was then assembled using Adobe® Photoshop® software for quality purposes.

Sporulation frequency counting

To visualize hyphal growth and sporulation defects during mating assays, the mating plates were directly observed under a Nikon Eclipse E400 microscope. Hyphal growth and basidia images were captured using the top-mounted Nikon DXM1200F camera on the microscope. The images were processed using Fiji-ImageJ and assembled in Adobe® Photoshop® software.

For crosses involving wild-type H99α, VYD135α, KN99**a**, Bt63**a**, IUM96**a**, approximately 1000 total basidia were counted after 4 weeks of mating, and the sporulation frequency was calculated. For crosses involving VYD135 *dmc1*Δ strain, three mating spots were setup independently. From each mating spot periphery, 6 images were captured after 3-4 weeks of mating. Basidia (both sporulating and non-sporulating) in each of these spots were counted manually after some processing of images using ImageJ. The sporulation frequency was determined by dividing the sporulating basidia by the total number of basidia for each spot. Each mating spot was considered as an independent experiment and at least 3000 basidia were counted from each mating spot.

Flow cytometry

Flow cytometry analysis was performed as described previously (Fu & Heitman, 2017). Cells were grown on YPD medium for two days at 30°C, harvested, and washed with 1X PBS buffer followed by fixation in 70% ethanol at 4°C overnight. Next, cells were washed once with 1 ml of NS buffer (10 mM Tris-HCl, pH = 7.2, 250 mM sucrose, 1 mM EDTA, pH = 8.0, 1 mM MgCl2, 0.1 mM CaCl2, 0.1 mM ZnCl2, 0.4 mM phenylmethylsulfonyl fluoride, and 7 mM β-mercaptoethanol), and finally resuspended in 180 µl NS buffer containing 20 µl 10 mg/ml RNase and 5 µl 0.5 mg/ml propidium iodide (PI) at 37°C for 3-4 hours. Then, 50 µl stained cells were diluted in 2 ml of 50 mM Tris-HCl, pH = 8.0, transferred to FACS compatible tube, and submitted for analysis at the Duke Cancer Institute Flow Cytometry Shared Resource. For each sample, 10,000 cells were analyzed on the FL1 channel on the Becton-Dickinson FACScan. Wild-type H99 and previously generated AI187 were used as haploid and diploid controls,

respectively, in these experiments. Data analysis was performed using the FlowJo software (RRID:SCR_008520).

Data Availability

The sequence data generated in this study were submitted to NCBI with the BioProject accession number PRJNA682203.

Acknowledgments

We thank Shelby Priest and Arti Dumbrepatil for the critical reading of this manuscript. This work was supported by NIH/NIAID R01 award AI39115-24, R01 grant AI50113-16 awarded to JH, and R01 grant AI33654-04 awarded to JH, David Tobin, and Paul Magwene. JH is also Co-Director and Fellow of the CIFAR program *Fungal Kingdom: Threats & Opportunities*.

Competing interests

The authors declare no competing interests.

References

Arras, S. D. M., Chitty, J. L., Blake, K. L., Schulz, B. L., & Fraser, J. A. (2015). A genomic safe haven for mutant complementation in *Cryptococcus neoformans*. *PLoS One, 10*(4). doi:10.1371/journal.pone.0122916

Avise, J. C. (2015). Evolutionary perspectives on clonal reproduction in vertebrate animals. *Proc Natl Acad Sci U S A, 112*(29), 8867-8873. doi:10.1073/pnas.1501820112

Booth, W., Smith, C. F., Eskridge, P. H., Hoss, S. K., Mendelson, J. R., 3rd, & Schuett, G. W. (2012). Facultative parthenogenesis discovered in wild vertebrates. *Biol Lett, 8*(6), 983-985. doi:10.1098/rsbl.2012.0666

Cimino, M. C. (1972a). Egg-production, polyploidization and evolution in a diploid all-female fish of the genus *Poeciliopsis*. *Evolution, 26*(2), 294-306. doi:10.1111/j.1558-5646.1972.tb00195.x

Cimino, M. C. (1972b). Meiosis in triploid all-female fish (*Poeciliopsis*, Poeciliidae). *Science, 175*(4029), 1484-1486. doi:10.1126/science.175.4029.1484

606 Conde, J., & Fink, G. R. (1976). A mutant of *Saccharomyces cerevisiae* defective for nuclear
607 fusion. *Proc Natl Acad Sci U S A, 73*(10), 3651-3655. doi:10.1073/pnas.73.10.3651
608 Dedukh, D., Litvinchuk, J., Svinin, A., Litvinchuk, S., Rosanov, J., & Krasikova, A. (2019).
609 Variation in hybridogenetic hybrid emergence between populations of water frogs from
610 the *Pelophylax esculentus* complex. *PLoS One, 14*(11), e0224759.
611 doi:10.1371/journal.pone.0224759
612 Dedukh, D., Majtanova, Z., Marta, A., Psenicka, M., Kotusz, J., Klima, J., . . . Janko, K. (2020).
613 Parthenogenesis as a solution to hybrid sterility: The mechanistic basis of meiotic
614 distortions in clonal and sterile hybrids. *Genetics, 215*(4), 975-987.
615 doi:10.1534/genetics.119.302988
616 Desjardins, C. A., Giamberardino, C., Sykes, S. M., Yu, C. H., Tenor, J. L., Chen, Y., . . .
617 Cuomo, C. A. (2017). Population genomics and the evolution of virulence in the fungal
618 pathogen *Cryptococcus neoformans*. *Genome Res, 27*(7), 1207-1219.
619 doi:10.1101/gr.218727.116
620 Dimijian, G. G. (2005). Evolution of sexuality: Biology and behavior. *Proc (Bayl Univ Med*
621 *Cent), 18*(3), 244-258. doi:10.1080/08998280.2005.11928075
622 Dolezalkova, M., Sember, A., Marec, F., Rab, P., Plotner, J., & Choleva, L. (2016). Is premeiotic
623 genome elimination an exclusive mechanism for hemiclonal reproduction in hybrid males
624 of the genus *Pelophylax*? *BMC Genet, 17*(1), 100. doi:10.1186/s12863-016-0408-z
625 Fan, Y., & Lin, X. (2018). Multiple applications of a transient CRISPR-Cas9 coupled with
626 electroporation (TRACE) system in the *Cryptococcus neoformans* species complex.
627 *Genetics, 208*(4), 1357-1372. doi:10.1534/genetics.117.300656
628 Fields, A. T., Feldheim, K. A., Poulakis, G. R., & Chapman, D. D. (2015). Facultative
629 parthenogenesis in a critically endangered wild vertebrate. *Curr Biol, 25*(11), R446-447.
630 doi:10.1016/j.cub.2015.04.018
631 Fraser, J. A., Giles, S. S., Wenink, E. C., Geunes-Boyer, S. G., Wright, J. R., Diezmann, S., . . .
632 Heitman, J. (2005). Same-sex mating and the origin of the Vancouver Island
633 *Cryptococcus gattii* outbreak. *Nature, 437*(7063), 1360-1364. doi:10.1038/nature04220
634 Fu, C., & Heitman, J. (2017). PRM1 and KAR5 function in cell-cell fusion and karyogamy to
635 drive distinct bisexual and unisexual cycles in the *Cryptococcus* pathogenic species
636 complex. *PLOS Genetics, 13*(11). doi:10.1371/journal.pgen.1007113

637 Heitman, J. (2015). Evolution of sexual reproduction: A view from the Fungal Kingdom supports
638 an evolutionary epoch with sex before sexes. *Fungal Biol Rev, 29*(3-4), 108-117.
639 doi:10.1016/j.fbr.2015.08.002
640 Heitman, J., Sun, S., & James, T. Y. (2013). Evolution of fungal sexual reproduction. *Mycologia,*
641 *105*(1), 1-27. doi:10.3852/12-253
642 Heppich, S., Tunner, H. G., & Greilhuber, J. (1982). Premeiotic chromosome doubling after
643 genome elimination during spermatogenesis of the species hybrid *Rana esculenta*. *Theor*
644 *Appl Genet, 61*(2), 101-104. doi:10.1007/BF00273874
645 Hodač, L., Klatt, S., Hojsgaard, D., Sharbel, T. F., & Hörandl, E. (2019). A little bit of sex
646 prevents mutation accumulation even in apomictic polyploid plants. *BMC Evolutionary*
647 *Biology, 19*(1). doi:10.1186/s12862-019-1495-z
648 Hojsgaard, D., & Harandl, E. (2015). A little bit of sex matters for genome evolution in asexual
649 plants. *Frontiers in Plant Science, 6*. doi:10.3389/fpls.2015.00082
650 Holsbeek, G., & Jooris, R. (2009). Potential impact of genome exclusion by alien species in the
651 hybridogenetic water frogs (*Pelophylax esculentus* complex). *Biological Invasions, 12*(1),
652 1. doi:10.1007/s10530-009-9427-2
653 Hörandl, E. (2009). Geographical parthenogenesis: Opportunities for asexuality. In I. Schön, K.
654 Martens, & P. Dijk (Eds.), *Lost Sex: The Evolutionary Biology of Parthenogenesis* (pp.
655 161-186). Dordrecht: Springer Netherlands.
656 Hurst, L. D., & Nurse, P. (1991). A note on the evolution of meiosis. *Journal of Theoretical*
657 *Biology, 150*(4), 561-563. doi:10.1016/s0022-5193(05)80447-3
658 Idnurm, A. (2010). A tetrad analysis of the basidiomycete fungus *Cryptococcus neoformans*.
659 *Genetics, 185*(1), 153-163. doi:10.1534/genetics.109.113027
660 Keller, S. M., Viviani, M. A., Esposto, M. C., Cogliati, M., & Wickes, B. L. (2003). Molecular
661 and genetic characterization of a serotype A *MAT*a *Cryptococcus neoformans* isolate.
662 *Microbiology, 149*(Pt 1), 131-142. doi:10.1099/mic.0.25921-0
663 Kozubowski, L., & Heitman, J. (2010). Septins enforce morphogenetic events during sexual
664 reproduction and contribute to virulence of *Cryptococcus neoformans*. *Molecular*
665 *Microbiology, 75*(3), 658-675. doi:10.1111/j.1365-2958.2009.06983.x

Kwon-Chung, K. J. (1975). A new genus, *filobasidiella*, the perfect state of *Cryptococcus neoformans*. *Mycologia, 67*(6), 1197-1200. Retrieved from https://www.ncbi.nlm.nih.gov/pubmed/765816

Kwon-Chung, K. J. (1976). Morphogenesis of *Filobasidiella neoformans*, the sexual state of *Cryptococcus neoformans*. *Mycologia, 68*(4), 821-833. Retrieved from https://www.ncbi.nlm.nih.gov/pubmed/790172

Lancashire, W. E., & Mattoon, J. R. (1979). Cytoduction: A tool for mitochondrial genetic studies in yeast. *Mol Gen Genet, 170*(3), 333-344. doi:10.1007/BF00267067

Lavanchy, G., & Schwander, T. (2019). Hybridogenesis. *Curr Biol, 29*(1), R9-R11. doi:10.1016/j.cub.2018.11.046

Lee, S. C., Ni, M., Li, W., Shertz, C., & Heitman, J. (2010). The evolution of sex: A perspective from the fungal kingdom. *Microbiol Mol Biol Rev, 74*(2), 298-340. doi:10.1128/MMBR.00005-10

Lehtonen, J., Schmidt, D. J., Heubel, K., & Kokko, H. (2013). Evolutionary and ecological implications of sexual parasitism. *Trends Ecol Evol, 28*(5), 297-306. doi:10.1016/j.tree.2012.12.006

Lin, X., Hull, C. M., & Heitman, J. (2005). Sexual reproduction between partners of the same mating type in *Cryptococcus neoformans*. *Nature, 434*(7036), 1017-1021. doi:10.1038/nature03448

Litvintseva, A. P., Marra, R. E., Nielsen, K., Heitman, J., Vilgalys, R., & Mitchell, T. G. (2003). Evidence of sexual recombination among *Cryptococcus neoformans* serotype A isolates in sub-Saharan Africa. *Eukaryot Cell, 2*(6), 1162-1168. doi:10.1128/ec.2.6.1162-1168.2003

Meirmans, S. (2009). The evolution of the problem of sex. In I. Schön, K. Martens, & P. Dijk (Eds.), *Lost Sex: The Evolutionary Biology of Parthenogenesis* (pp. 21-46). Dordrecht: Springer Netherlands.

Mirzaghaderi, G., & Horandl, E. (2016). The evolution of meiotic sex and its alternatives. *Proc Biol Sci, 283*(1838). doi:10.1098/rspb.2016.1221

Morrow, C. A., Lee, I. R., Chow, E. W., Ormerod, K. L., Goldinger, A., Byrnes, E. J., 3rd, . . . Fraser, J. A. (2012). A unique chromosomal rearrangement in the *Cryptococcus*

neoformans var. *grubii* type strain enhances key phenotypes associated with virulence. *mBio, 3*(2). doi:10.1128/mBio.00310-11

Nabais, C., Pereira, C., Cunado, N., & Collares-Pereira, M. J. (2012). Synaptonemal complexes in the hybridogenetic *Squalius alburnoides* fish complex: New insights on the gametogenesis of allopolyploids. *Cytogenet Genome Res, 138*(1), 31-35. doi:10.1159/000339522

Neaves, W. B., & Baumann, P. (2011). Unisexual reproduction among vertebrates. *Trends Genet, 27*(3), 81-88. doi:10.1016/j.tig.2010.12.002

Nielsen, K., Cox, G. M., Wang, P., Toffaletti, D. L., Perfect, J. R., & Heitman, J. (2003). Sexual cycle of *Cryptococcus neoformans* var. *grubii* and virulence of congenic **a** and alpha isolates. *Infect Immun, 71*(9), 4831-4841. doi:10.1128/iai.71.9.4831-4841.2003

Perfect, J. R., Ketabchi, N., Cox, G. M., Ingram, C. W., & Beiser, C. L. (1993). Karyotyping of *Cryptococcus neoformans* as an epidemiological tool. *J Clin Microbiol, 31*(12), 3305-3309. doi:10.1128/JCM.31.12.3305-3309.1993

Phadke, S. S., Feretzaki, M., Clancey, S. A., Mueller, O., & Heitman, J. (2014). Unisexual reproduction of *Cryptococcus gattii*. *PLoS One, 9*(10), e111089. doi:10.1371/journal.pone.0111089

Roth, C., Sun, S., Billmyre, R. B., Heitman, J., & Magwene, P. M. (2018). A high-resolution map of meiotic recombination in *Cryptococcus deneoformans* demonstrates decreased recombination in unisexual reproduction. *Genetics, 209*(2), 567-578. doi:10.1534/genetics.118.300996

Schwander, T., & Oldroyd, B. P. (2016). Androgenesis: Where males hijack eggs to clone themselves. *Philos Trans R Soc Lond B Biol Sci, 371*(1706). doi:10.1098/rstb.2015.0534

Soderlund, C., Bomhoff, M., & Nelson, W. M. (2011). SyMAP v3.4: a turnkey synteny system with application to plant genomes. *Nucleic Acids Res, 39*(10), e68. doi:10.1093/nar/gkr123

Sun, S., Billmyre, R. B., Mieczkowski, P. A., & Heitman, J. (2014). Unisexual reproduction drives meiotic recombination and phenotypic and karyotypic plasticity in *Cryptococcus neoformans*. *PLoS Genet, 10*(12), e1004849. doi:10.1371/journal.pgen.1004849

Sun, S., Coelho, M. A., David-Palma, M., Priest, S. J., & Heitman, J. (2019). The evolution of sexual reproduction and the mating-type locus: Links to pathogenesis of *Cryptococcus*

human pathogenic fungi. *Annu Rev Genet, 53*, 417-444. doi:10.1146/annurev-genet-120116-024755

Sun, S., Fu, C., Ianiri, G., & Heitman, J. (2020). The pheromone and pheromone receptor mating-type locus Is involved in controlling uniparental mitochondrial inheritance in *Cryptococcus*. *Genetics, 214*(3), 703-717. doi:10.1534/genetics.119.302824

Sun, S., Hoy, M. J., & Heitman, J. (2020). Fungal pathogens. *Curr Biol, 30*(19), R1163-R1169. doi:10.1016/j.cub.2020.07.032

Sun, S., Priest, S. J., & Heitman, J. (2019). *Cryptococcus neoformans* mating and genetic crosses. *Curr Protoc Microbiol, 53*(1), e75. doi:10.1002/cpmc.75

Tunner, H. G., & Heppich-Tunner, S. (1991). Genome exclusion and two strategies of chromosome duplication in oogenesis of a hybrid frog. *Naturwissenschaften, 78*(1), 32-34. doi:10.1007/BF01134041

Tunner, H. G., & Heppich, S. (1981). Premeiotic genome exclusion during oogenesis in the common edible frog, *Rana esculenta*. *Naturwissenschaften, 68*(4), 207-208. doi:10.1007/BF01047207

Umphrey, G. J. (2006). Sperm parasitism in ants: selection for interspecific mating and hybridization. *Ecology, 87*(9), 2148-2159. doi:10.1890/0012-9658(2006)87[2148:spiasf]2.0.co;2

Uzzell, T., Günther, R., & Berger, L. (1976). *Rana ridibunda* and *Rana esculenta*: A Leaky Hybridogenetic System (Amphibia Salientia). *Proceedings of the Academy of Natural Sciences of Philadelphia, 128*, 147-171. doi:https://www.jstor.org/stable/4064723

Vinogradov, A. E., Borkin, L. J., Gunther, R., & Rosanov, J. M. (1991). Two germ cell lineages with genomes of different species in one and the same animal. *Hereditas, 114*(3), 245-251. doi:10.1111/j.1601-5223.1991.tb00331.x

Wilkins, A. S., & Holliday, R. (2009). The evolution of meiosis from mitosis. *Genetics, 181*(1), 3-12. doi:10.1534/genetics.108.099762

Yadav, V., & Sanyal, K. (2018). Sad1 spatiotemporally regulates kinetochore clustering to ensure high-fidelity chromosome segregation in the human fungal pathogen *Cryptococcus neoformans*. *mSphere, 3*(4). doi:10.1128/mSphere.00190-18

Yadav, V., Sun, S., Coelho, M. A., & Heitman, J. (2020). Centromere scission drives chromosome shuffling and reproductive isolation. *Proc Natl Acad Sci U S A, 117*(14), 7917-7928. doi:10.1073/pnas.1918659117

Zakharov, I. A., & Yarovoy, B. P. (1977). Cytoduction as a new tool in studying the cytoplasmic heredity in yeast. *Mol Cell Biochem, 14*(1-3), 15-18. doi:10.1007/BF01734159

Zhao, Y., Lin, J., Fan, Y., & Lin, X. (2019). Life cycle of *Cryptococcus neoformans*. *Annu Rev Microbiol, 73*, 17-42. doi:10.1146/annurev-micro-020518-120210

Table 1. Genotype analysis of basidia-specific spores germinated from H99α x KN99a and VYD135α x KN99a crosses.

Basidia #	H99α x KN99**a** cross				VYD135α x KN99**a** cross			
	Spores germinated/ dissected	**% germinated**	***MAT***	**Mito**	**Spores germinated/ dissected**	**% germinated**	***MAT***	**Mito**
1	5/14	36	4α + 1**a**	**a**	12/24	50	All α	**a**
2	14/14	100	7α + 7**a**	**a**	6/10	60	All α	**a**
3	12/14	86	2α + 7**a** +3**a**/α	**a**	15/15	100	All **a**	**a**
4	10/14	71	4α +6**a**	**a**	22/27	81	All **a**	**a**
5	7/13	54	6**a** + 1**a**/α	**a**	3/12	25	All α	**a**
6	13/14	93	6α + 7**a**	**a**	25/27	93	All α	**a**
7	11/14	79	6α + 5**a**	**a**	4/4	100	All α	**a**
8	14/14	100	12α + 2**a**	**a**	10/13	77	All α	**a**
9	10/14	71	4α + 6**a**	**a**	13/15	87	All α	**a**
10	14/14	100	7α + 7**a**	**a**	31/61	51	All α	**a**
11	14/14	100	10α + 4**a**	**a**	10/10	100	All **a**	**a**
12	12/14	86	8α + 4**a**	**a**	4/5	80	All **a**	**a**
13	4/11	36	All **a**	**a**	24/28	86	All **a**	**a**
14	13/13	100	8α + 5**a**	**a**	16/28	57	All **a**	**a**
15	14/14	100	7α + 7**a**	**a**	11/11	100	All **a**	**a**
16	14/14	100	6α + 8**a**	**a**	10/22	45	All α	**a**

Mito refers to Mitochondria.

Figures and Figure Legends

Figure 1. Chromosome shuffled strain exhibits unusual sexual reproduction. (A-B) Images of cultures for the individual strains H99α, KN99**a**, and VYD135α, showing no self-filamentation on mating medium. Magnification=10X. **(C-D)** Light microscopy images showing robust sporulation in the H99α x KN99**a** cross, whereas the VYD135α x KN99**a** cross exhibited robust hyphal development but infrequent sporulation events. The inset images in colored boxes show examples of basidia observed in each of the crosses. Bar, 100 µm. **(E-F)** A scheme showing the *MAT*α (H99α and VYD135α) and *MAT***a** (KN99**a**) alleles at the *STE20* **(E)** and *COX1* **(F)** loci. Primers used for PCR analysis are marked by blue triangles. **(G)** Gel images showing PCR amplification of *STE20* and *COX1* alleles in the progeny obtained from four different basidia for both H99α x KN99**a** and VYD135α x KN99**a** crosses. PCR analysis for the parental strains is also shown, and key bands for DNA marker are labeled.

Figure 2. Fluorescence microscopy reveals uniparental nuclear inheritance in the wild-type crosses. (A) Crosses of GFP-H4 tagged H99α and mCherry-H4 tagged KN99**a** revealed the presence of both fluorescent markers in most spore chains along with uniparental nuclear inheritance in rare cases (~1%). In these few sporulating basidia, only one of the fluorescent signals was observed in the spore chains, reflecting the presence of only one parental nucleus in these basidia. **(B)** Crosses involving GFP-H4 tagged VYD135α and mCherry-H4 tagged KN99**a** revealed the presence of spore chains with only one fluorescent color. In the majority of basidia that have both parental nuclei, marked by both GFP and mCherry signals, spore chains are not produced, consistent with a failure of meiosis in these basidia. Bars, 10 µm.

Figure 3. VYD135α progeny exhibit strict uniparental nuclear inheritance and lack the signature of meiotic recombination. (A) Chromosome maps for H99α/KN99**a**, VYD135α, Bt63**a**, and IUM96**a** showing the karyotype variation. The genome of the wild-type strain H99α served as the reference. Black arrowheads represent chromosome translocations between VYD135α and H99α whereas red arrowheads mark chromosomes with a translocation between H99α and Bt63**a** or IUM96**a**. **(B)** Whole-genome sequencing, followed by SNP identification, of H99α x Bt63**a** progeny revealed evidence of meiotic recombination in all of the progeny. The

left panel shows SNPs with respect to the Bt63**a** genome whereas the right panel depicts SNPs against the H99α genome. H99α and Bt63**a** Illumina sequencing data served as controls for SNP calling. **(C)** SNP analysis of VYD135α x Bt63**a** progeny revealed no contribution of the Bt63**a** parental genome in the progeny as evidenced by the presence of SNPs only against Bt63**a** (left panel) but not against the VYD135α genome (right panel). The presence of a few SNPs observed in VYD135α, as well as all VYD135α x Bt63**a** progeny, are within nucleotide repeat regions. GF stands for germination frequency and P stands for progeny. **(D)** SNP analysis of H99α x Bt63**a** and VYD135α x Bt63**a** progeny using mitochondrial DNA as the reference revealed that mitochondrial DNA is inherited from Bt63**a** in all of the progeny. Progeny obtained from VYD135α x Bt63**a** basidium 18 also revealed recombination between the two parental mitochondrial genomes as marked by the absence or presence of two SNPs when mapped against VYD135α and Bt63 mitochondrial genomes, respectively. The green bar in each panel depicts the locus used for PCR analysis of the mitochondrial genotype in the progeny.

Figure 4. Pan-hyphal microscopy reveals the loss of one parental nucleus during pseudosexual reproduction. Spore-producing long hyphae were visualized in both (**A**) wild-type H99α x KN99**a** and (**B**) VYD135α x KN99**a** crosses to study the dynamics of nuclei in hyphae. Both nuclei were present across the hyphal length in the wild-type and resulted in the production of recombinant spores. On the other hand, one of the nuclei was lost during hyphal branching in the VYD135α x KN99**a** cross and resulted in uniparental nuclear inheritance in the spores that were produced. The arrow in **B** marks the hyphal branching point after which only one of the parental nuclei is present (also see Figure 4-figure supplement 1A). The images were captured as independent sections and assembled to obtain the final presented image. Bars, 10 µm.

Figure 5. Meiotic recombinase Dmc1 is required for pseudosexual reproduction. (A) Light microscopy images showing the impact of *dmc1* mutation on sexual and pseudosexual reproduction in *C. neoformans*. Bar, 100 µm. **(B)** A graph showing quantification (n=3) of sporulation events in multiple crosses with *dmc1*Δ mutants. At least 3000 basidia were counted in each experiment.

Figure 6. Model for the role of pseudosexual reproduction in *C. neoformans* ecology. Scenarios showing possible roles for pseudosexual reproduction under various hypothetical mating conditions. Except for one condition where the two parents are completely compatible with each other, pseudosexual reproduction could play a significant role in survival and dissemination despite its occurrence at a low frequency.

Supplementary Figure Legends

Figure 2-figure supplement 1. Dynamics of sexual reproduction and sporulation analyzed with *C. neoformans* strains expressing nuclear-localized fluorescent reporter proteins. (A) A cartoon depicting various stages of sexual reproduction in *C. neoformans*, from the formation of conjugation tube to sporulation, and possible dynamics of the nuclei at these different stages. After cell-cell fusion, tagged proteins assort into both nuclei and yield a yellow/orange fluorescence color as a result of the mixing of the green and red signals. Cartoons in the box show hypothetical scenarios where uniparental nuclear inheritance occurs after the loss of one parental nucleus. **(B)** Direct fluorescence microscopy images showing the status of GFP-H4 and mCherry-H4 tagged nuclei in post-mating hyphae as well as in spores. Both GFP and mCherry fluorescent colors were observed in hyphae and spores as hypothesized in A. Bar, 10 μm.

Figure 2-figure supplement 2. Nuclear dynamics during sporulation in the wild-type and VYD135α crosses. GFP-H4 and mCherry-H4 tagging revealed different localization patterns in the **(A)** wild-type H99α x KN99**a** and **(B)** VYD135α x KN99**a** crosses. Wild-type spore chains mostly harbored both the nuclear stains as a result of bisexual meiosis. On the other hand, basidia with only one of the parental nuclei produced spores in VYD135α x KN99**a** crosses; basidia with both nuclei failed to produce spore chains and, as a result, remained as bald basidia. Bars, 10 μm.

Figure 3-figure supplement 1. Pseudosexual reproduction occurs in natural isolates, Bt63a and IUM96a. (A) Images of the mating spots showing filamentation when two strains of opposite mating-type are crossed. No filamentation is observed without the presence of a mating partner. **(B and D)** Light microscopy images showing sporulation frequency in crosses involving Bt63**a (B)** and IUM96**a (D)**. Bars, 100 μm. **(C and E)** Schemes depicting the *STE20* alleles used for *MAT* locus and *COB1* (for Bt63**a**) and *COX1* (for IUM96**a**) alleles for mitochondrial genotyping, respectively. Gel images show the PCR analysis on progeny from four basidia and the parental strains for all crosses as mentioned.

Figure 3-figure supplement 2. Bt63a fluorescence microscopy revealed pseudosexual reproduction events. GFP-H4 tagged VYD135α crossed with mCherry-H4 tagged Bt63**a** showed only VYD135α sporulation events as also observed in spore dissection analysis. Bars, 10 μm.

Figure 3-figure supplement 3. VYD135α x Bt63a progeny lack signatures of meiotic recombination. SNP analysis on VYD135α x Bt63**a** progeny revealed no contribution of the Bt63**a** parental genome in the progeny as evidenced by the presence of SNPs only against Bt63**a** (left panel) but not against VYD135α genome (right panel). The few SNPs observed in VYD135 as well as all VYD135α x Bt63**a** progeny lie within nucleotide repeat regions. GF stands for germination frequency and P stands for progeny.

Figure 3-figure supplement 4. Mitochondria are inherited from *MAT*a parent in all of the progeny. (A) A map of SNPs detected in H99α x Bt63**a** progeny when using H99α mitochondrial DNA (upper panel) and Bt63**a** mitochondrial DNA (lower panel) as the reference. **(B)** SNP analysis revealed variants in all the progeny when using VYD135α mitochondrial DNA as the reference but not when using Bt63**a** mitochondrial DNA. The two SNPs detected against Bt63**a** DNA in progeny P19-24 (Basidium 18) suggest recombination of two parental mitochondrial DNA during mating. The green bar in each panel depicts the fragment used for PCR analysis in Figure 3-figure supplement 1. P stands for progeny.

Figure 3-figure supplement 5. VYD135α x Bt63a progeny are haploid. (A) Whole-genome sequencing of the H99α x Bt63**a** progeny revealed extensive aneuploidy in the progeny. Each progeny seemed to exhibit aneuploidy for at least one chromosome. **(B)** Whole-genome sequencing data revealed that the progeny obtained from VYD135α x Bt63**a** 5-week old crosses are euploid in nature as they show a uniform level of genomic content when mapped to the Bt63 genome. VYD135α and Bt63**a** whole-genome sequencing data were also mapped as controls. Each lane represents one strain, and the difference in intensity correlates with the number of reads obtained per sample. **(C)** Flow-cytometry analysis on progeny obtained from three basidia confirmed that all the germinating progeny are haploid. While progeny from B12 and B14 are

the same as used for the whole-genome sequencing, progeny from B3 were subjected to only flow cytometry analysis. Bt63**a** and VYD135α were also analyzed as controls for this experiment. P stands for progeny.

Figure 3-figure supplement 6. IUM96a exhibits meiotic recombination in progeny with H99α but not with the genome shuffle strain VYD135α. (A) The left panel depicts SNPs with respect to the IUM96**a** genome whereas the right panel shows SNPs against the H99α genome. Whole-genome sequencing, followed by SNP analysis, for the H99α x IUM96**a** progeny (basidia 3 and 4) revealed evidence of meiotic recombination in the progeny. Basidium 7 from the H99α x IUM96**a** cross produced uniparental progeny, which was confirmed by SNP analysis on a subset of these progeny. The progeny exhibited SNPs only against the IUM96**a** genome but not against the H99α genome. **(B)** SNP analysis from two different basidia revealed inheritance of only one set of parental nuclear DNA in the progeny from VYD135α x IUM96**a** cross. Basidium 3 progeny possessed DNA from only the VYD135α parent, while basidium 5 progeny inherited nuclear DNA from IUM96**a** alone. The results obtained from this analysis are congruent with mating-type PCR results shown in Supplementary file 1b. GF stands for germination frequency and P stands for progeny.

Figure 3-figure supplement 7. Ploidy analysis of IUM96a progeny reveals haploid uniparental progeny. Whole-genome sequencing analysis revealed the presence of multiple aneuploidies in the **(A)** H99α x IUM96**a** progeny, but a completely euploid genome for the **(B)** VYD135α x IUM96**a** progeny. P stands for progeny.

Figure 4-figure supplement 1. Hyphal branches act as a gateway for nuclear separation during pseudosexual reproduction. (A) Individual z-sections showing the hyphal branching (marked by arrow) where the two parental nuclei segregate in the figure 4B. **(B)** Images showing hyphal branching points where one of the parental nuclei separates from the main hyphae with two parental nuclei (Top two panels). The branch point is marked with the arrow. The lower two panels show the long hyphae with only one of the parental nuclei in them. The third panel shows other hyphae with both parental nuclei suggesting that separation occurred at an early stage. The

fourth panel exhibits the same between VYD135α x Bt63**a** but also has a sporulating basidium on it. Bar, 10 μm.

Figure 5-figure supplement 1. Dmc1 deletion leads to severe sporulation defects in both sexual and pseudosexual reproduction. Light microscopy images showing the phenotype of *DMC1* deletion in **(A)** H99α x KN99**a** unilateral crosses as well as bilateral mutant crosses and **(B)** VYD135α x KN99**a** *dmc1*Δ unilateral and bilateral crosses. The deletion of *DMC1* led to a reduction in sporulating basidia in bilateral mutant crosses.

Figure 5-figure supplement 2. Meiotic regulator Dmc1 is required for pseudosexual reproduction. A cross between a GFP-H4 tagged VYD135α strain and an mCherry-H4 tagged KN99**a** *dmc1*Δ mutant revealed that Dmc1 is required for pseudosexual reproduction events. The majority of the KN99**a** *dmc1*Δ nucleus-containing basidia failed to produce spore chains (top two rows and bottom rows). While all 11 observed basidia with VYD135α nuclei produced spores, only 2 out of 19 observed basidia with KN99**a** *dmc1*Δ nuclei produced spores. One of these two is represented in the third row. Bars, 10 μm.

Figure 6-figure supplement 1. Unisexual, bisexual and pseudosexual reproduction in *C. neoformans*. A diagram depicting various types of sexual reproduction in *Cryptococcus* species. *C. deneoformans* exhibits unisexual reproduction in which two cells of the same mating-type fuse or a single cell undergoes endoreplication followed by the production of clonal progeny. Both *C. neoformans* and *C. deneoformans* show bisexual reproduction in which two cells of opposite mating-types fuse with each other and produce recombinant progeny. Pseudosexual reproduction, as proposed in this study, arises from bisexual mating but generates clonal progeny of one of the parents after the other parental nucleus is lost during development. While both unisexual and pseudosexual reproduction produce clonal progeny, they differ with respect to the inheritance of mitochondrial DNA (marked by grey color cell background in the illustration).

Supplementary File 1a. The genotype of basidia-specific spores dissected from H99α x Bt63a and VYD135α x Bt63a crosses.

Supplementary File 1b. The genotype of basidia-specific spores dissected from H99α x IUM96-2828a and VYD135α x IUM96-2828a crosses.

Supplementary File 1c. Genotype analysis of basidia-specific progeny from H99α *dmc1*Δ x KN99a *dmc1*Δ and VYD135α *dmc1*Δ x KN99a *dmc1*Δ crosses.

Supplementary File 1d. Strains used in this study.

Supplementary File 1e. Primers used in this study.

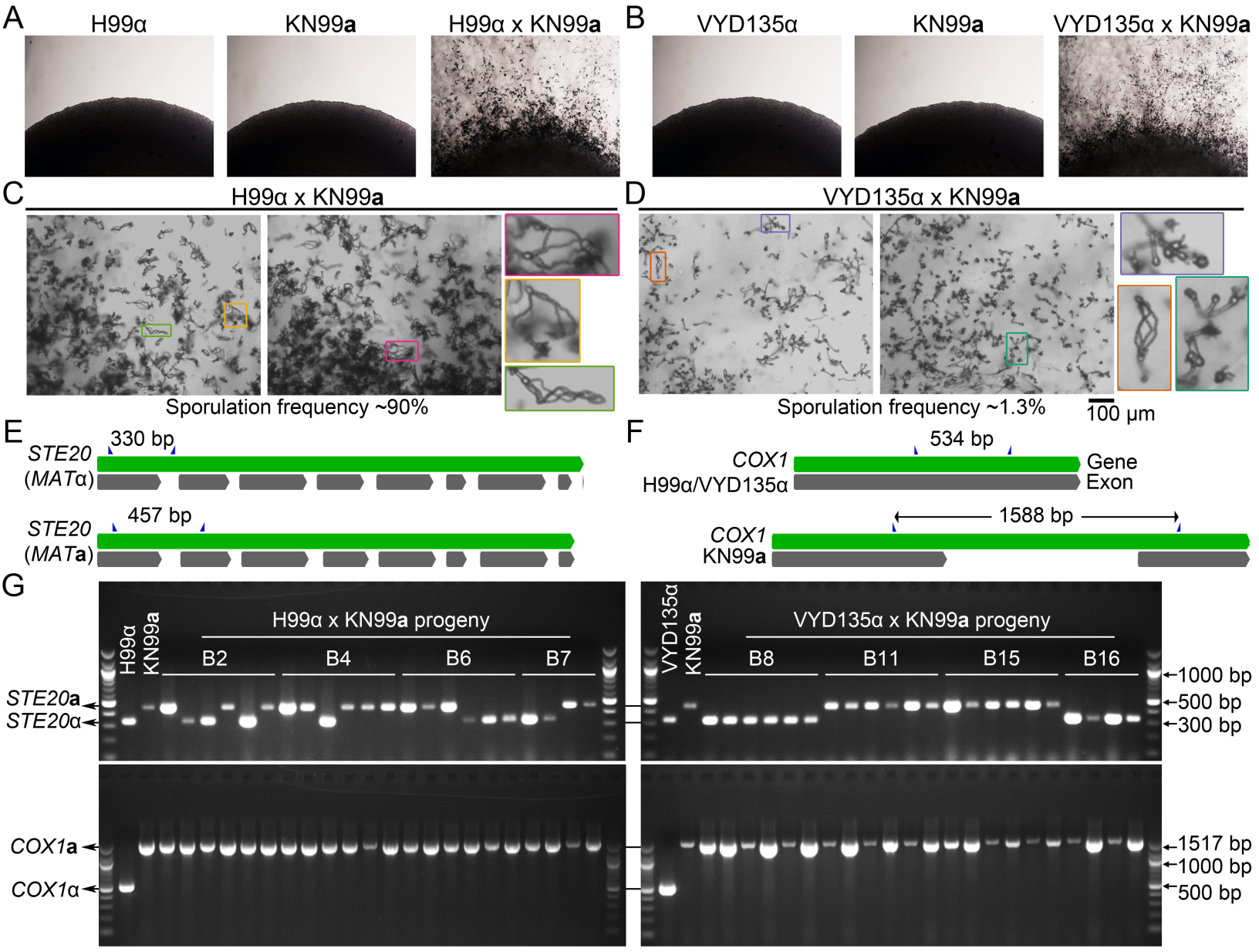
A
H99α
KN99a
H99α x KN99a
B
VYD135α
KN99a
VYD135α x KN99a
C
H99α x KN99a
Sporulation frequency ~90%
D
VYD135α x KN99a
Sporulation frequency ~1.3%
100 μm
E
330 bp
STE20
(MATα)
457 bp
STE20
(MATa)
F
534 bp
COX1
H99α/VYD135α
Gene
Exon
1588 bp
COX1
KN99a
G
H99α
KN99a
H99α x KN99a progeny
B2
B4
B6
B7
VYD135α
KN99a
VYD135α x KN99a progeny
B8
B11
B15
B16
STE20a
STE20α
1000 bp
500 bp
300 bp
COX1a
COX1α
1517 bp
1000 bp
500 bp

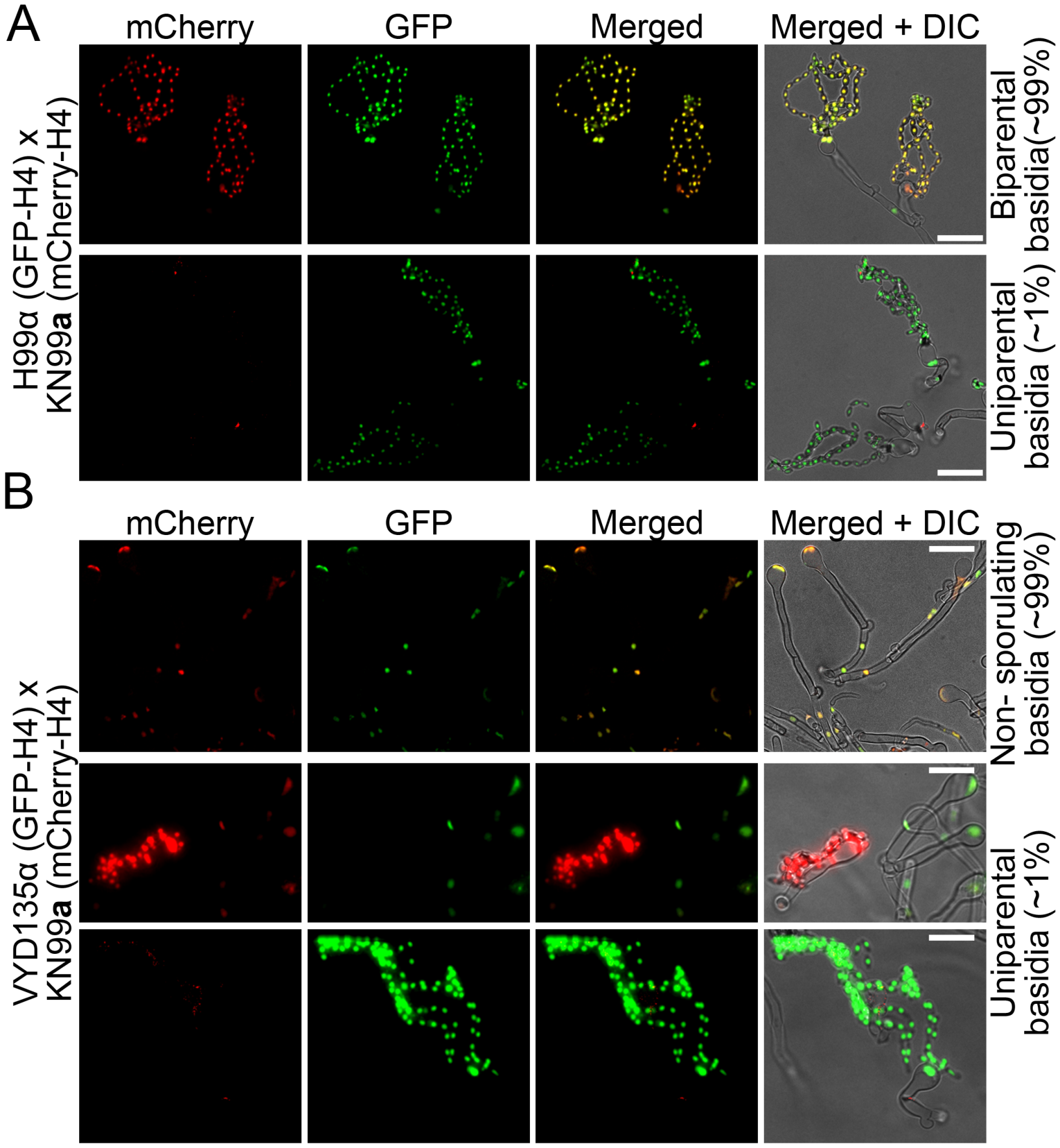
A
mCherry
GFP
Merged
Merged + DIC
H99α (GFP-H4) x
KN99**a** (mCherry-H4)
Biparental
basidia(~99%)
Uniparental
basidia (~1%)
B
mCherry
GFP
Merged
Merged + DIC
VYD135α (GFP-H4) x
KN99**a** (mCherry-H4)
Non- sporulating
basidia (~99%)
Uniparental
basidia (~1%)

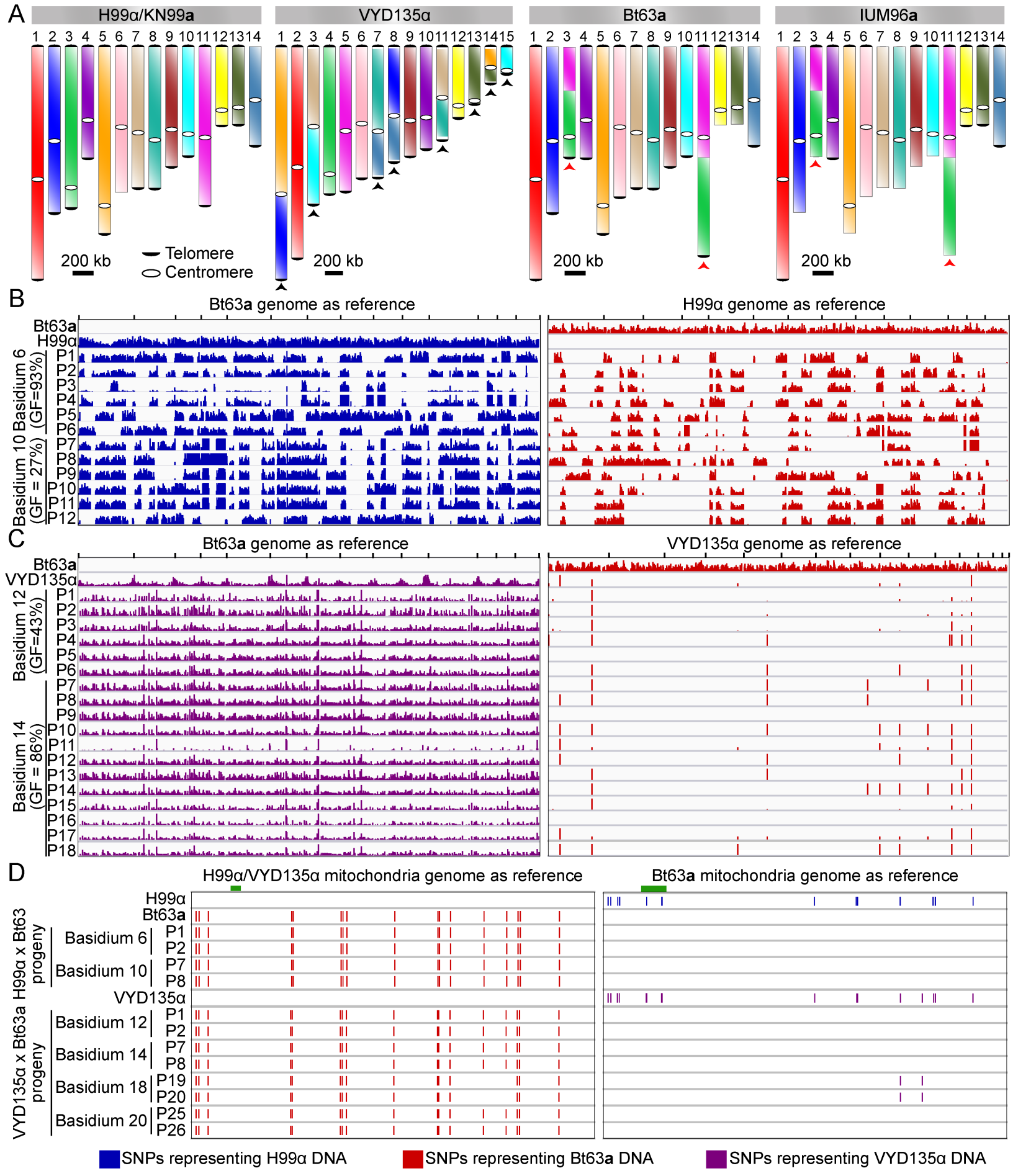
A
H99α/KN99a
VYD135α
Bt63a
IUM96a
200 kb
Telomere
Centromere
B
Bt63a genome as reference
H99α genome as reference
Bt63a
H99α
Basidium 6 (GF=93%)
Basidium 10 (GF = 27%)
P1
P2
P3
P4
P5
P6
P7
P8
P9
P10
P11
P12
C
Bt63a genome as reference
VYD135α genome as reference
Bt63a
VYD135α
Basidium 12 (GF=43%)
Basidium 14 (GF = 86%)
P1
P2
P3
P4
P5
P6
P7
P8
P9
P10
P11
P12
P13
P14
P15
P16
P17
P18
D
H99α/VYD135α mitochondria genome as reference
Bt63a mitochondria genome as reference
H99α
Bt63a
H99α x Bt63 progeny
Basidium 6
Basidium 10
P1
P2
P7
P8
VYD135α
VYD135α x Bt63a progeny
Basidium 12
Basidium 14
Basidium 18
Basidium 20
P1
P2
P7
P8
P19
P20
P25
P26
SNPs representing H99α DNA
SNPs representing Bt63a DNA
SNPs representing VYD135α DNA

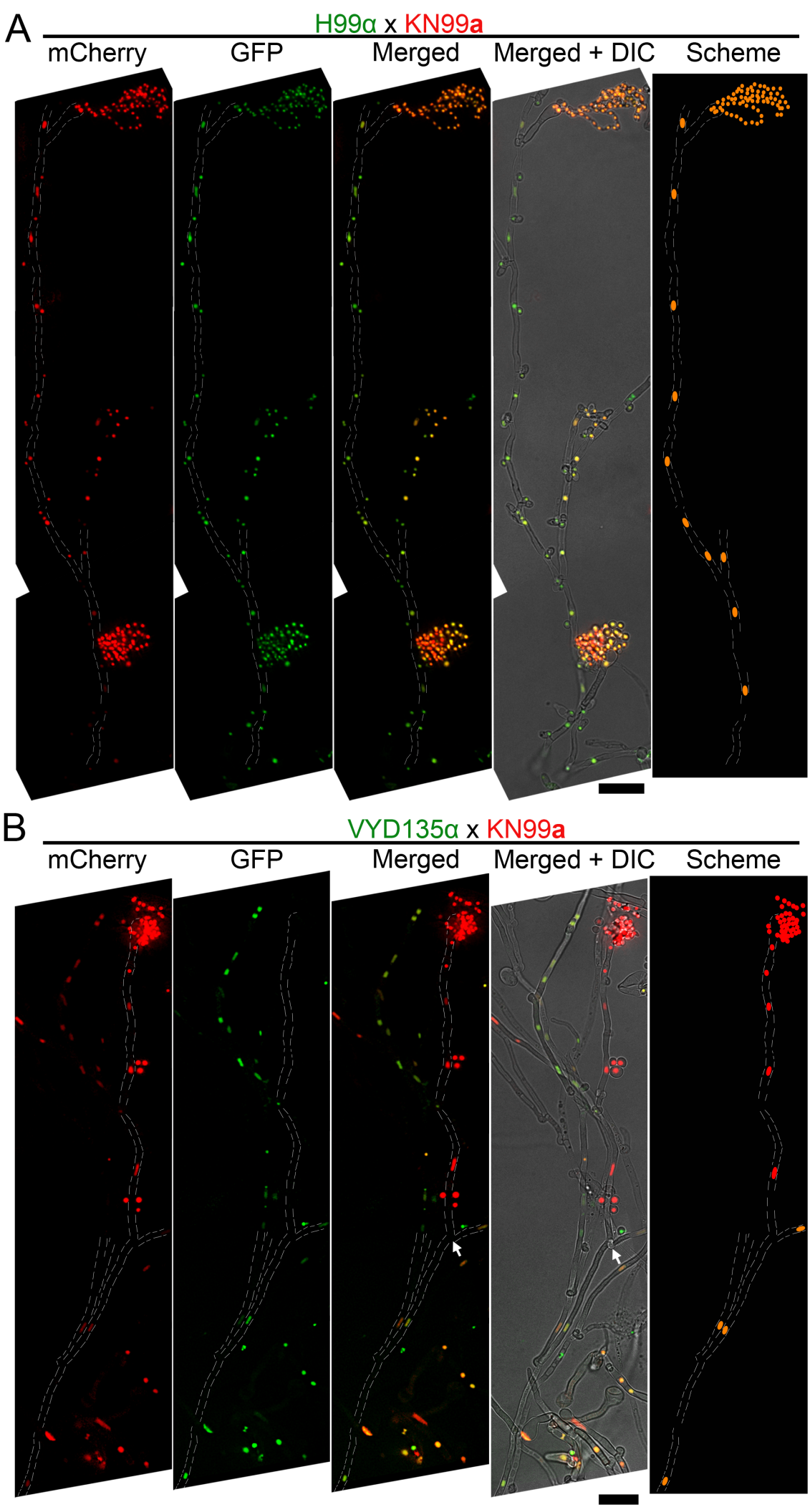
A
H99α x KN99a
mCherry
GFP
Merged
Merged + DIC
Scheme
B
VYD135α x KN99a
mCherry
GFP
Merged
Merged + DIC
Scheme

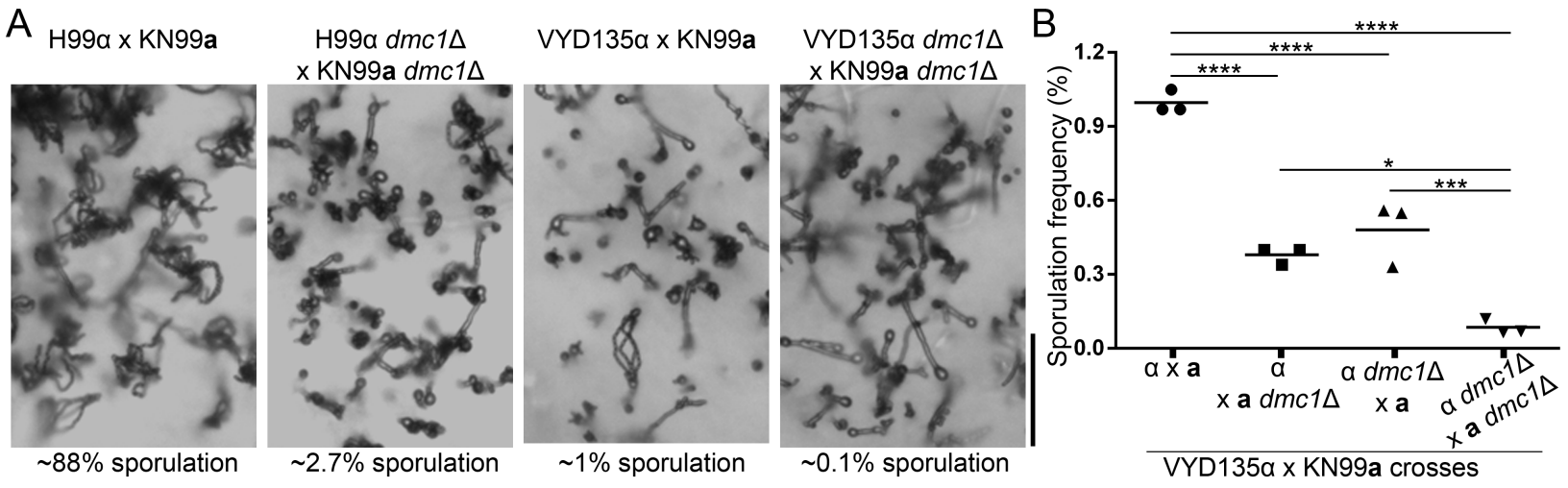
A
H99α x KN99**a**
H99α *dmc1*Δ x KN99**a** *dmc1*Δ
VYD135α x KN99**a**
VYD135α *dmc1*Δ x KN99**a** *dmc1*Δ
~88% sporulation
~2.7% sporulation
~1% sporulation
~0.1% sporulation
B
Sporulation frequency (%)
1.2
0.9
0.6
0.3
0.0
****
****
****
*
***
α x **a**
α x **a** *dmc1*Δ
α *dmc1*Δ x **a**
α *dmc1*Δ x **a** *dmc1*Δ
VYD135α x KN99**a** crosses

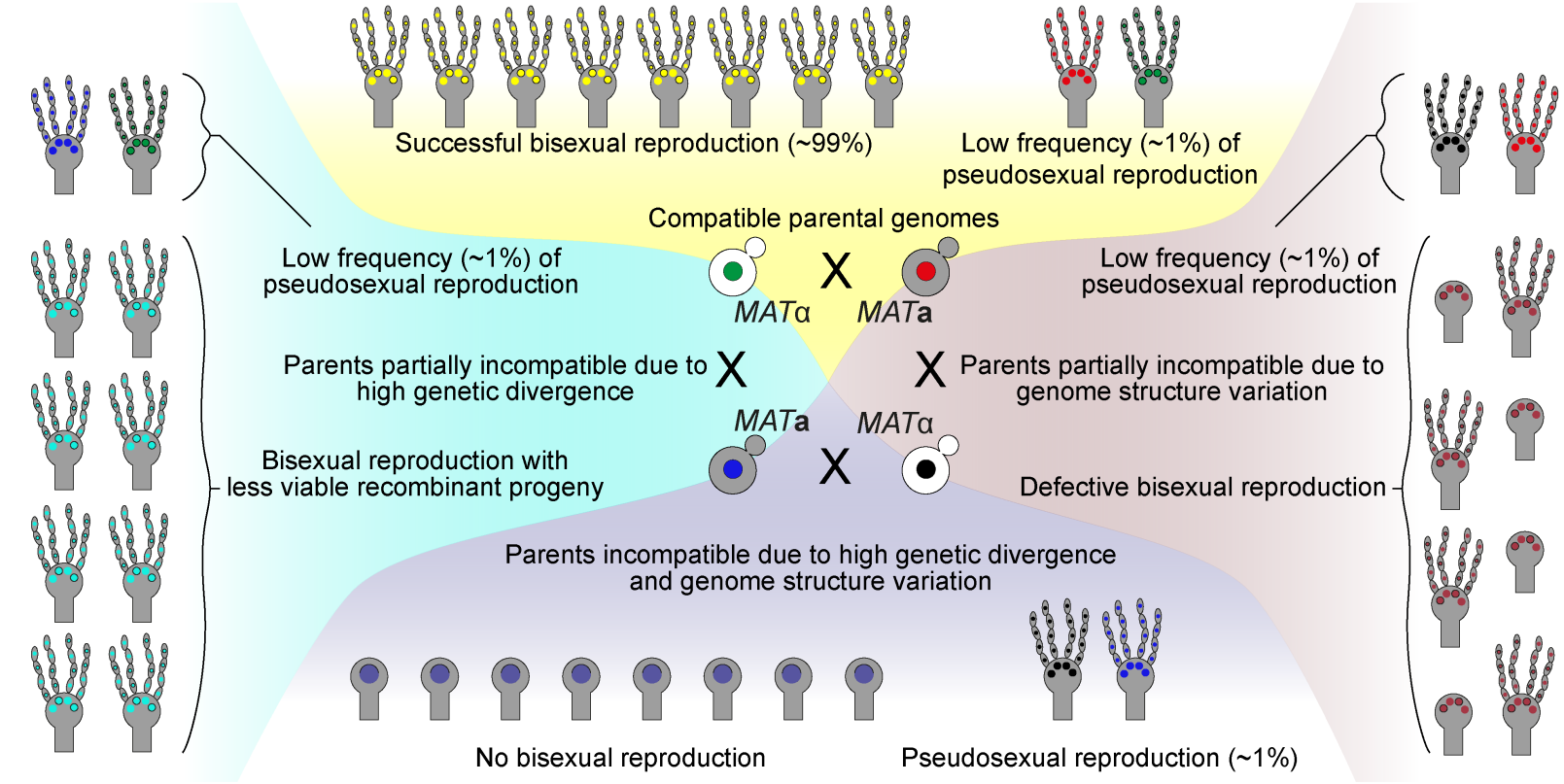
Successful bisexual reproduction (~99%)
Low frequency (~1%) of pseudosexual reproduction
Compatible parental genomes
Low frequency (~1%) of pseudosexual reproduction
MATα
MATa
Low frequency (~1%) of pseudosexual reproduction
Parents partially incompatible due to high genetic divergence
Parents partially incompatible due to genome structure variation
MATa
MATα
Bisexual reproduction with less viable recombinant progeny
Defective bisexual reproduction
Parents incompatible due to high genetic divergence and genome structure variation
No bisexual reproduction
Pseudosexual reproduction (~1%)

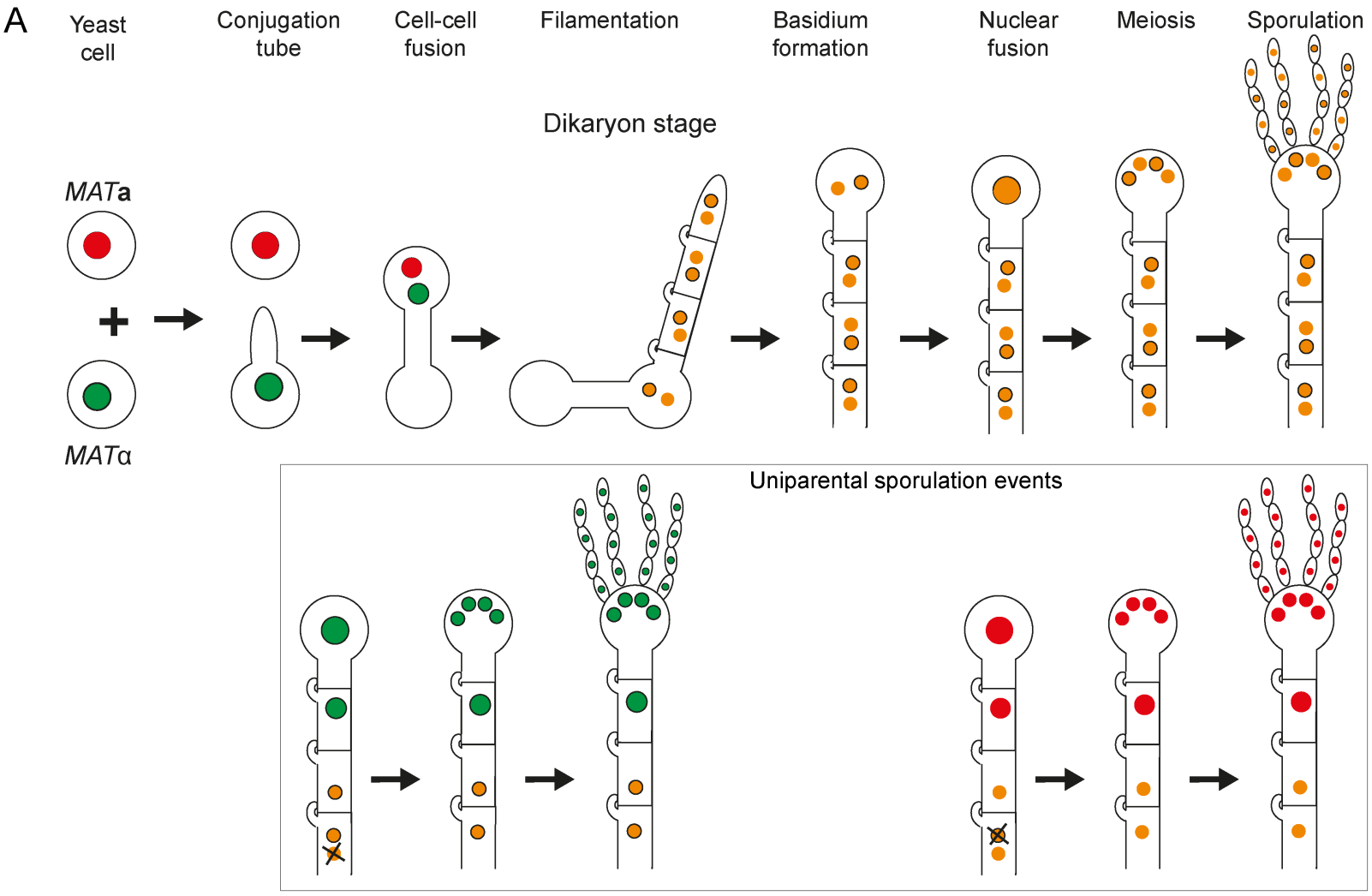
A
Yeast cell
Conjugation tube
Cell-cell fusion
Filamentation
Basidium formation
Nuclear fusion
Meiosis
Sporulation
Dikaryon stage
MATa
MATα
Uniparental sporulation events

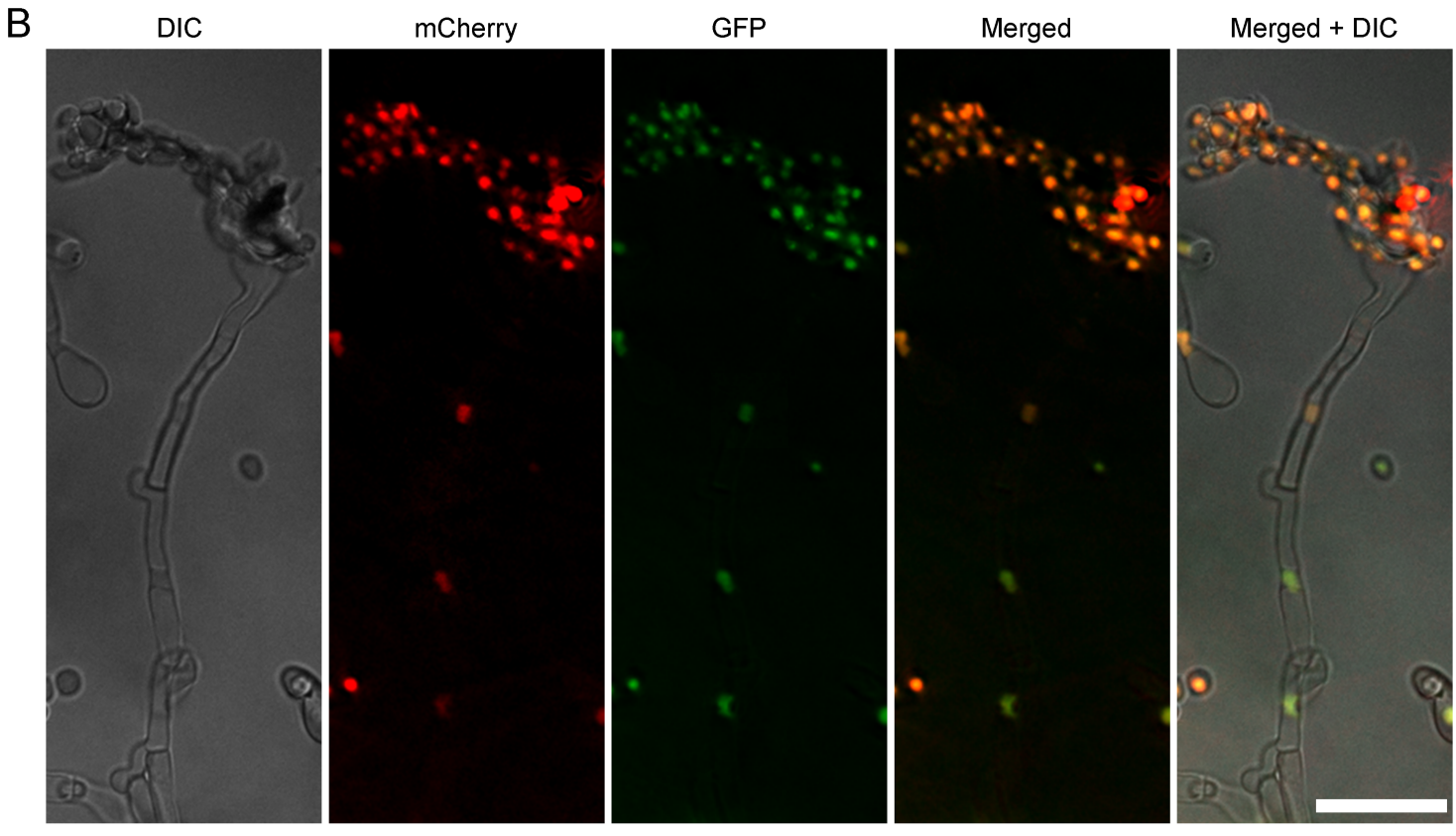
B
DIC
mCherry
GFP
Merged
Merged + DIC

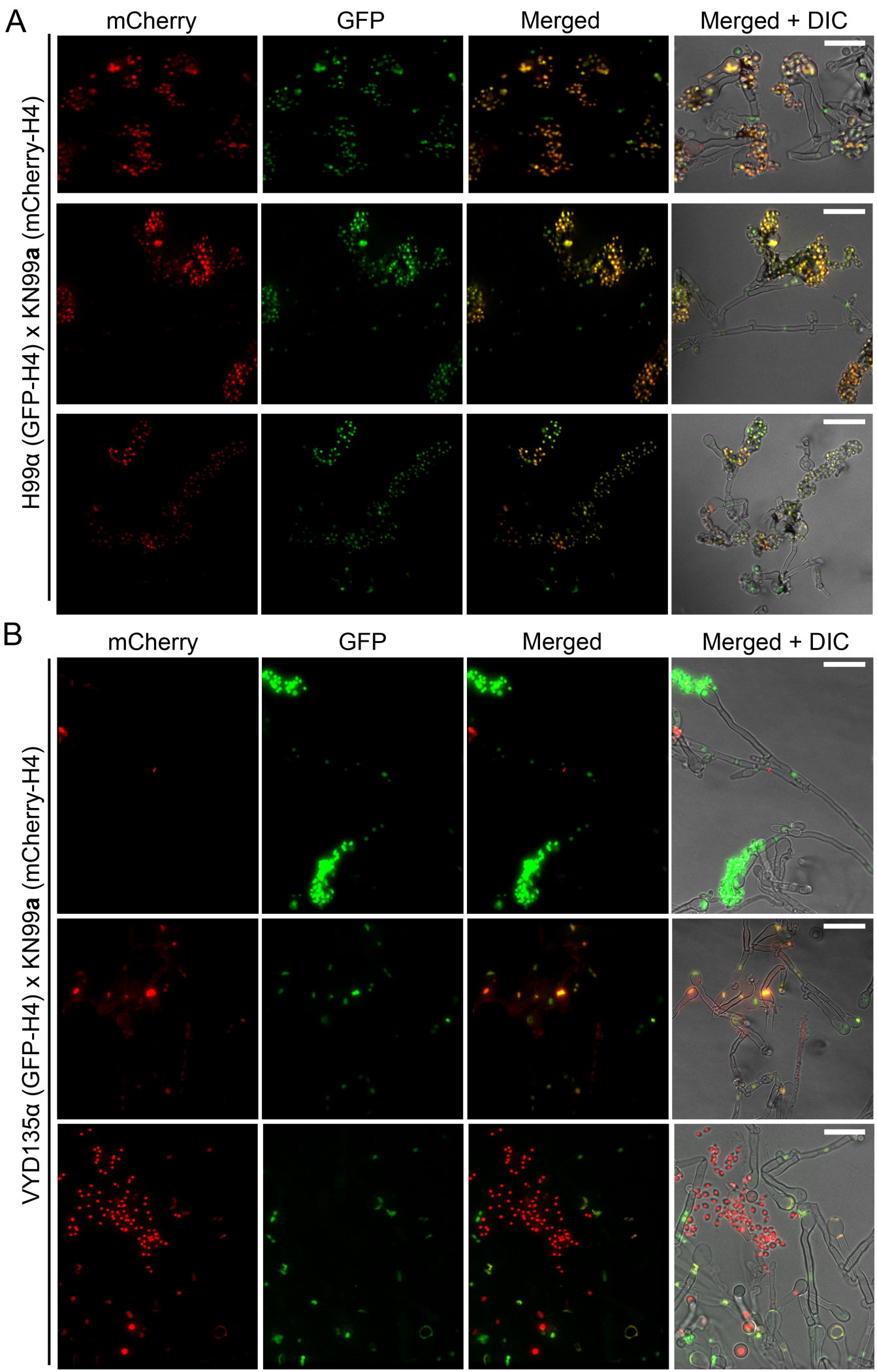
A
mCherry
GFP
Merged
Merged + DIC
H99α (GFP-H4) x KN99a (mCherry-H4)
B
mCherry
GFP
Merged
Merged + DIC
VYD135α (GFP-H4) x KN99a (mCherry-H4)

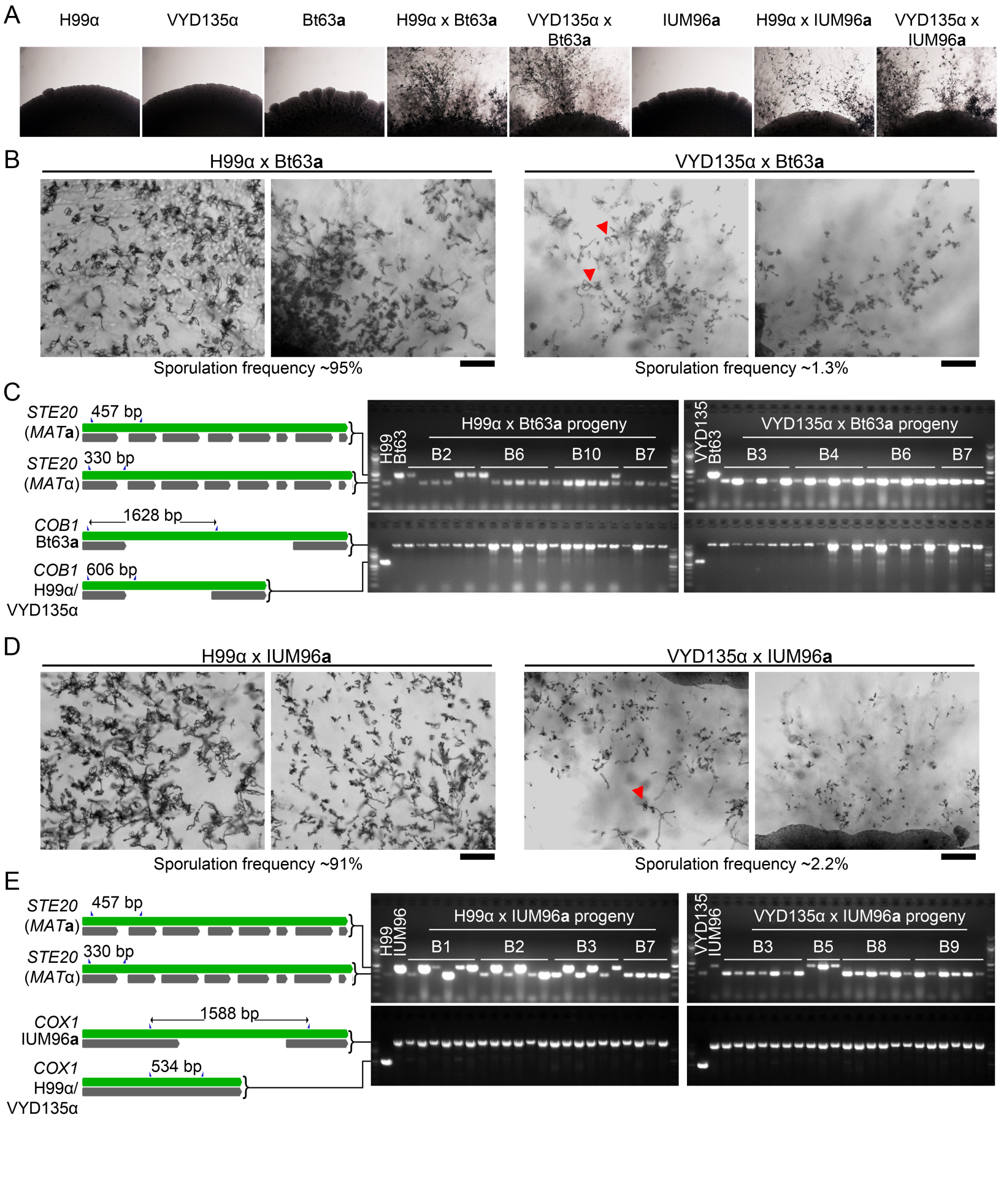
A
H99α
VYD135α
Bt63a
H99α x Bt63a
VYD135α x Bt63a
IUM96a
H99α x IUM96a
VYD135α x IUM96a
B
H99α x Bt63a
VYD135α x Bt63a
Sporulation frequency ~95%
Sporulation frequency ~1.3%
C
STE20 (MATa) 457 bp
STE20 (MATα) 330 bp
COB1 Bt63a 1628 bp
COB1 H99α/ VYD135α 606 bp
H99 Bt63
H99α x Bt63a progeny
B2
B6
B10
B7
VYD135 Bt63
VYD135α x Bt63a progeny
B3
B4
B6
B7
D
H99α x IUM96a
VYD135α x IUM96a
Sporulation frequency ~91%
Sporulation frequency ~2.2%
E
STE20 (MATa) 457 bp
STE20 (MATα) 330 bp
COX1 IUM96a 1588 bp
COX1 H99α/ VYD135α 534 bp
H99 IUM96
H99α x IUM96a progeny
B1
B2
B3
B7
VYD135 IUM96
VYD135α x IUM96a progeny
B3
B5
B8
B9

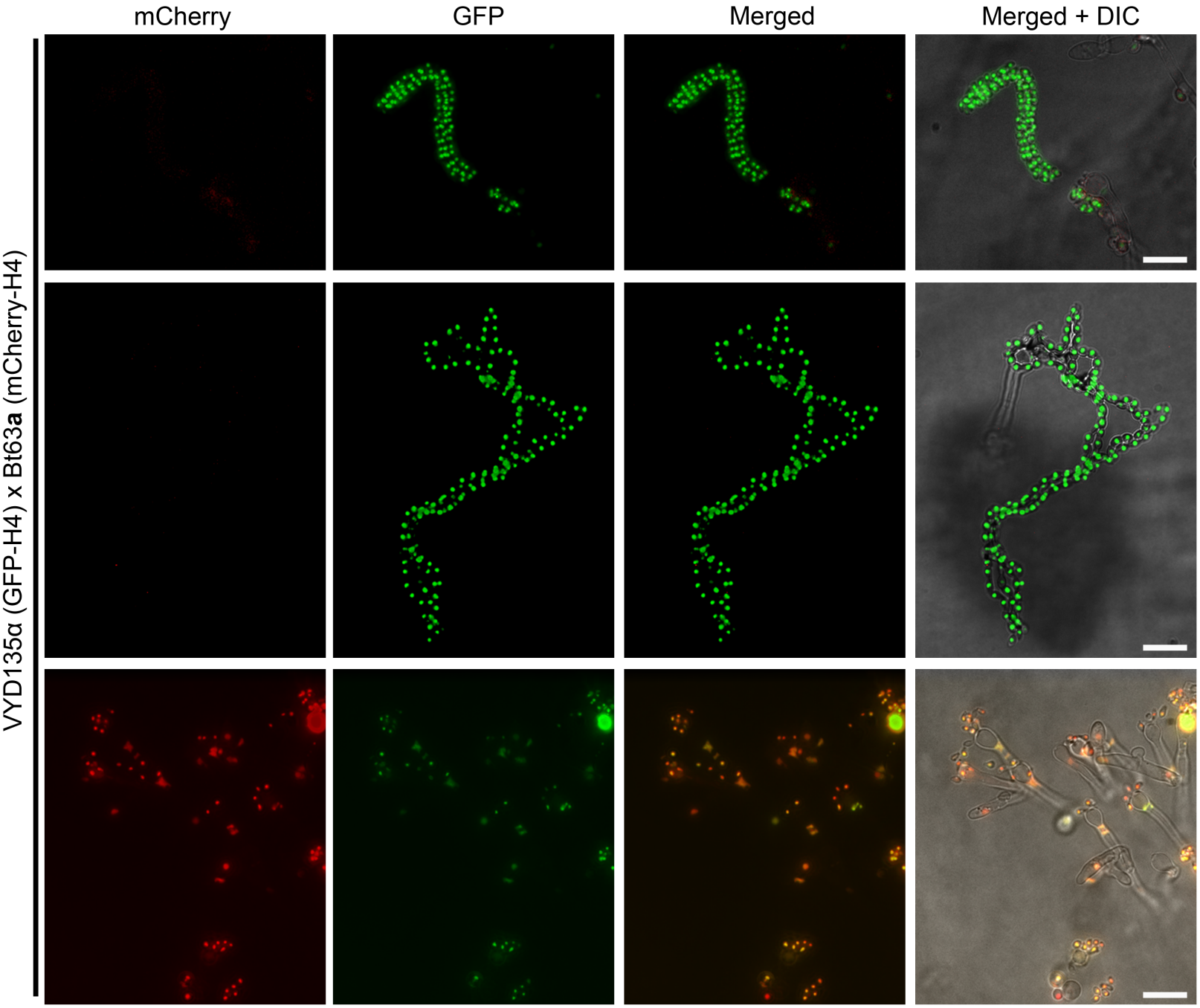
mCherry
GFP
Merged
Merged + DIC
VYD135α (GFP-H4) x Bt63**a** (mCherry-H4)

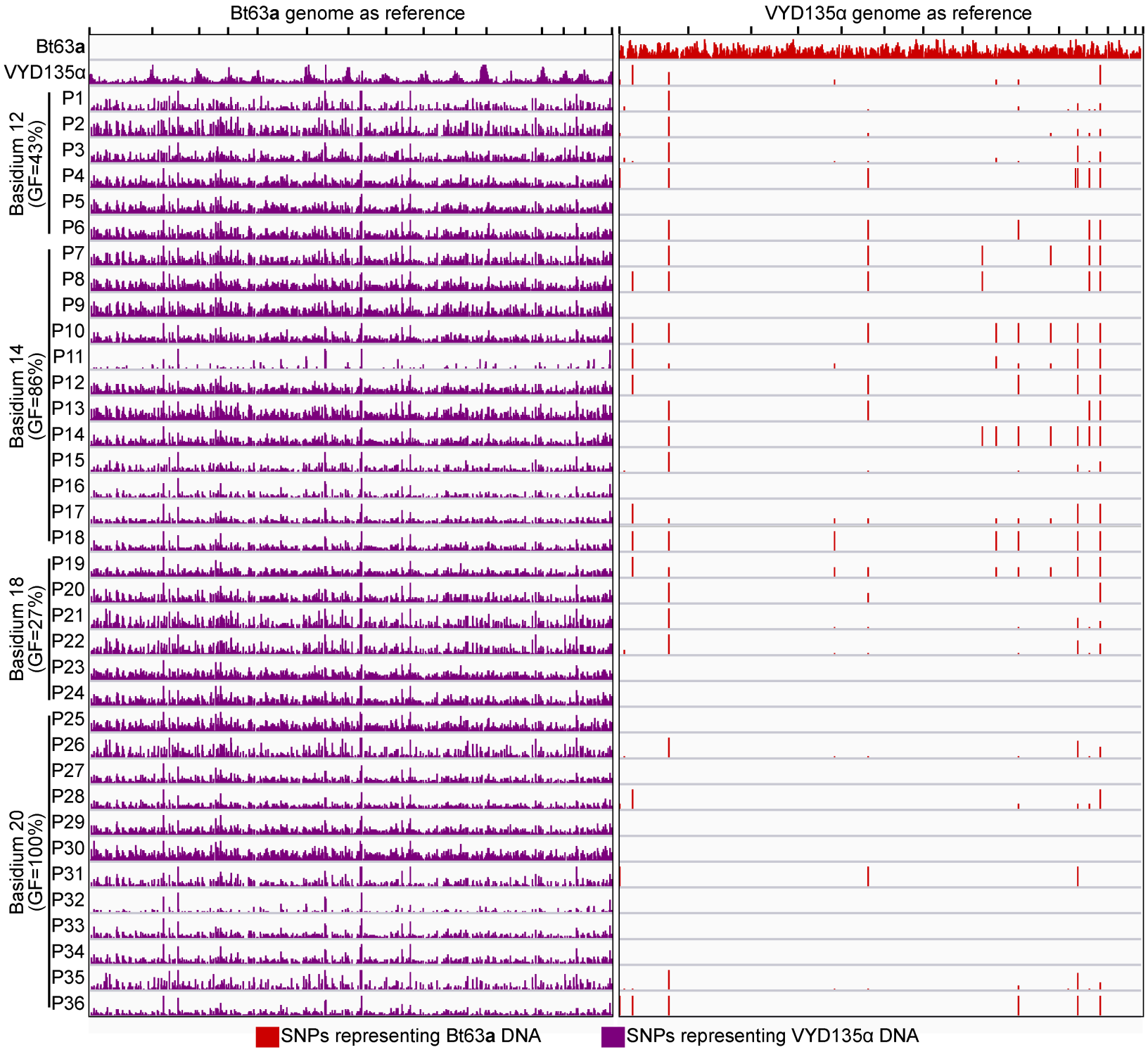
Bt63a genome as reference
VYD135α genome as reference
Bt63a
VYD135α
Basidium 12 (GF=43%)
P1
P2
P3
P4
P5
P6
Basidium 14 (GF=86%)
P7
P8
P9
P10
P11
P12
P13
P14
P15
P16
P17
P18
Basidium 18 (GF=27%)
P19
P20
P21
P22
P23
P24
Basidium 20 (GF=100%)
P25
P26
P27
P28
P29
P30
P31
P32
P33
P34
P35
P36
SNPs representing Bt63a DNA
SNPs representing VYD135α DNA

A

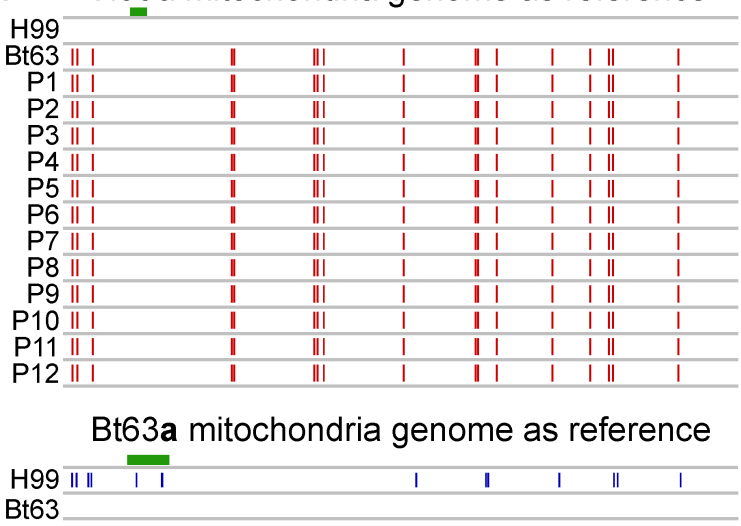

No SNPs detected in the H99 x Bt63 progeny when using Bt63 mitochondrial genome as reference.

B

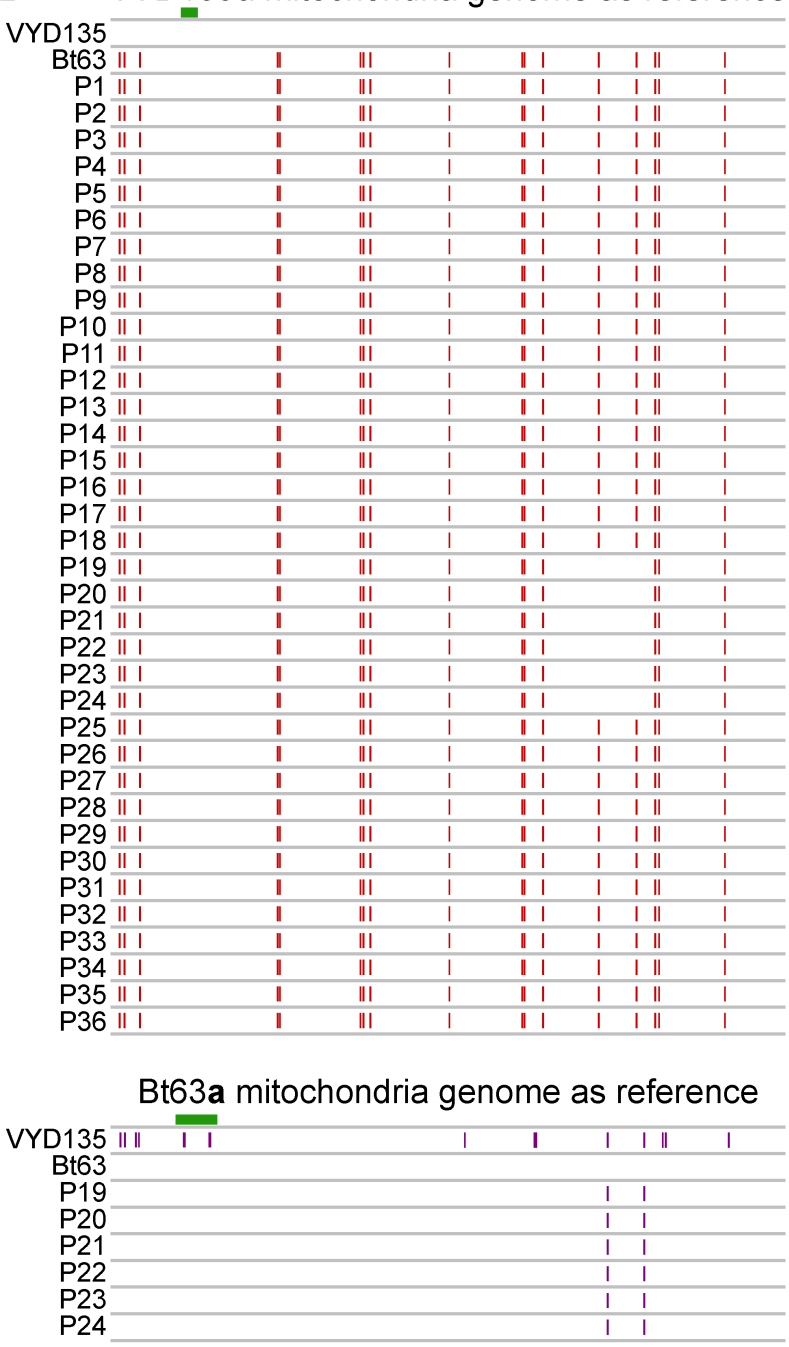

No SNPs detected in rest of the VYD135 x Bt63 progeny when using Bt63 mitochondrial genome as reference.

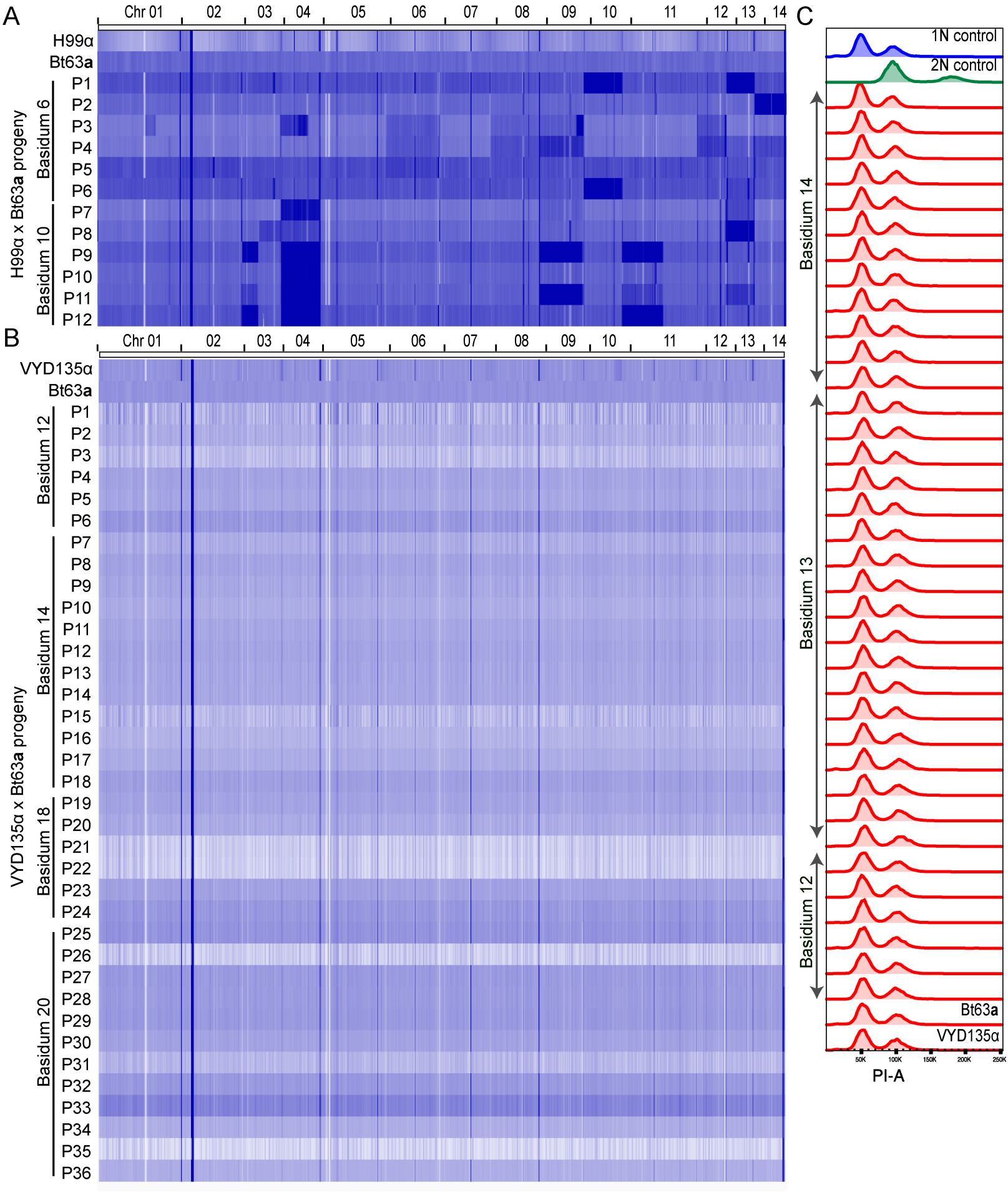
A
Chr 01
02
03
04
05
06
07
08
09
10
11
12
13
14
H99α
Bt63a
H99α x Bt63a progeny
Basidum 6
P1
P2
P3
P4
P5
P6
Basidum 10
P7
P8
P9
P10
P11
P12
B
VYD135α
Bt63a
VYD135α x Bt63a progeny
Basidum 12
Basidum 14
Basidum 18
Basidum 20
P13
P14
P15
P16
P17
P18
P19
P20
P21
P22
P23
P24
P25
P26
P27
P28
P29
P30
P31
P32
P33
P34
P35
P36
C
1N control
2N control
Basidium 14
Basidium 13
Basidium 12
Bt63a
VYD135α
50K
100K
150K
200K
250K
PI-A

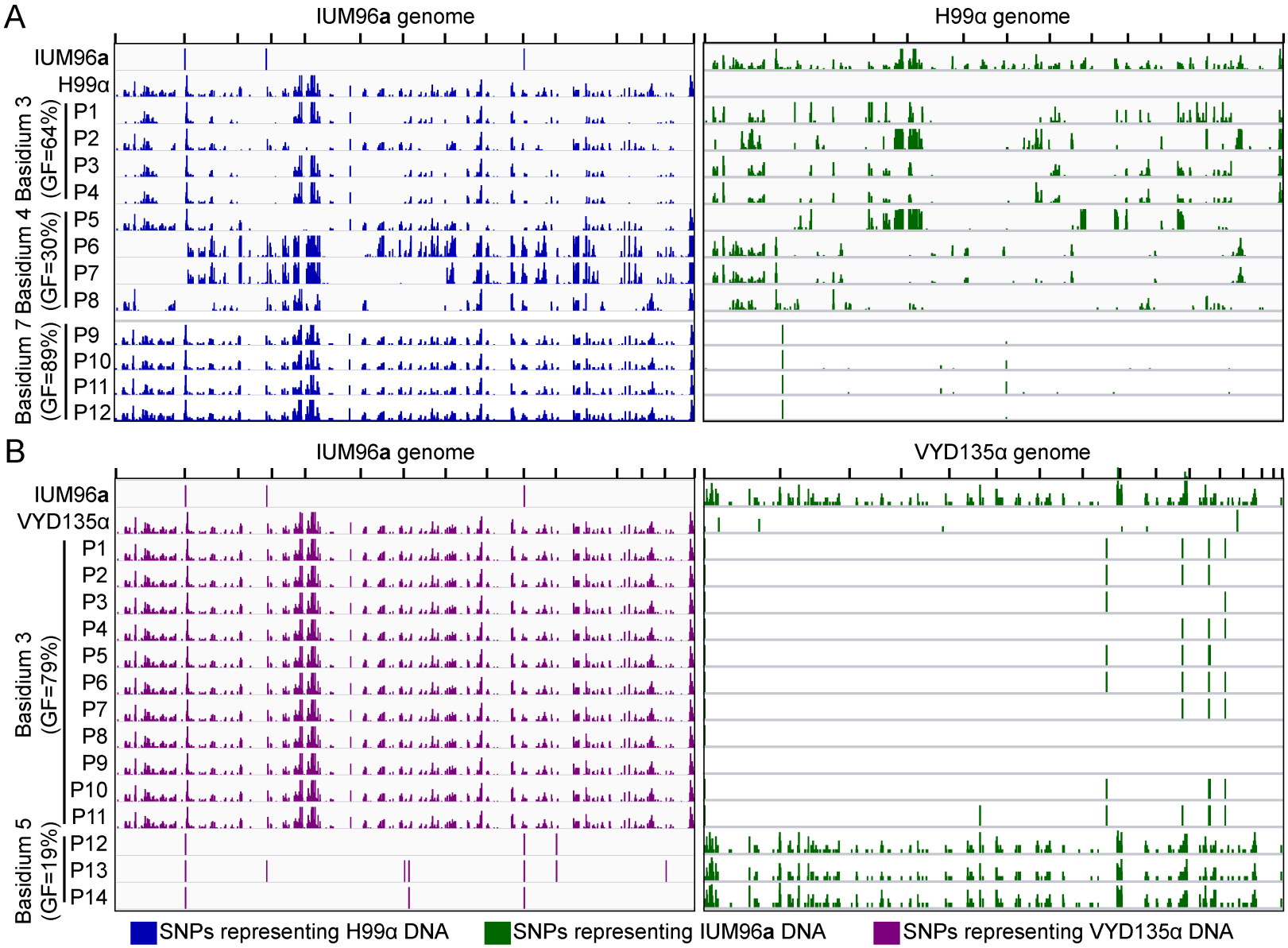
A
IUM96a genome
H99α genome
IUM96a
H99α
Basidium 3 (GF=64%)
P1
P2
P3
P4
Basidium 4 (GF=30%)
P5
P6
P7
P8
Basidium 7 (GF=89%)
P9
P10
P11
P12
B
IUM96a genome
VYD135α genome
IUM96a
VYD135α
Basidium 3 (GF=79%)
P1
P2
P3
P4
P5
P6
P7
P8
P9
P10
P11
Basidium 5 (GF=19%)
P12
P13
P14
SNPs representing H99α DNA
SNPs representing IUM96a DNA
SNPs representing VYD135α DNA

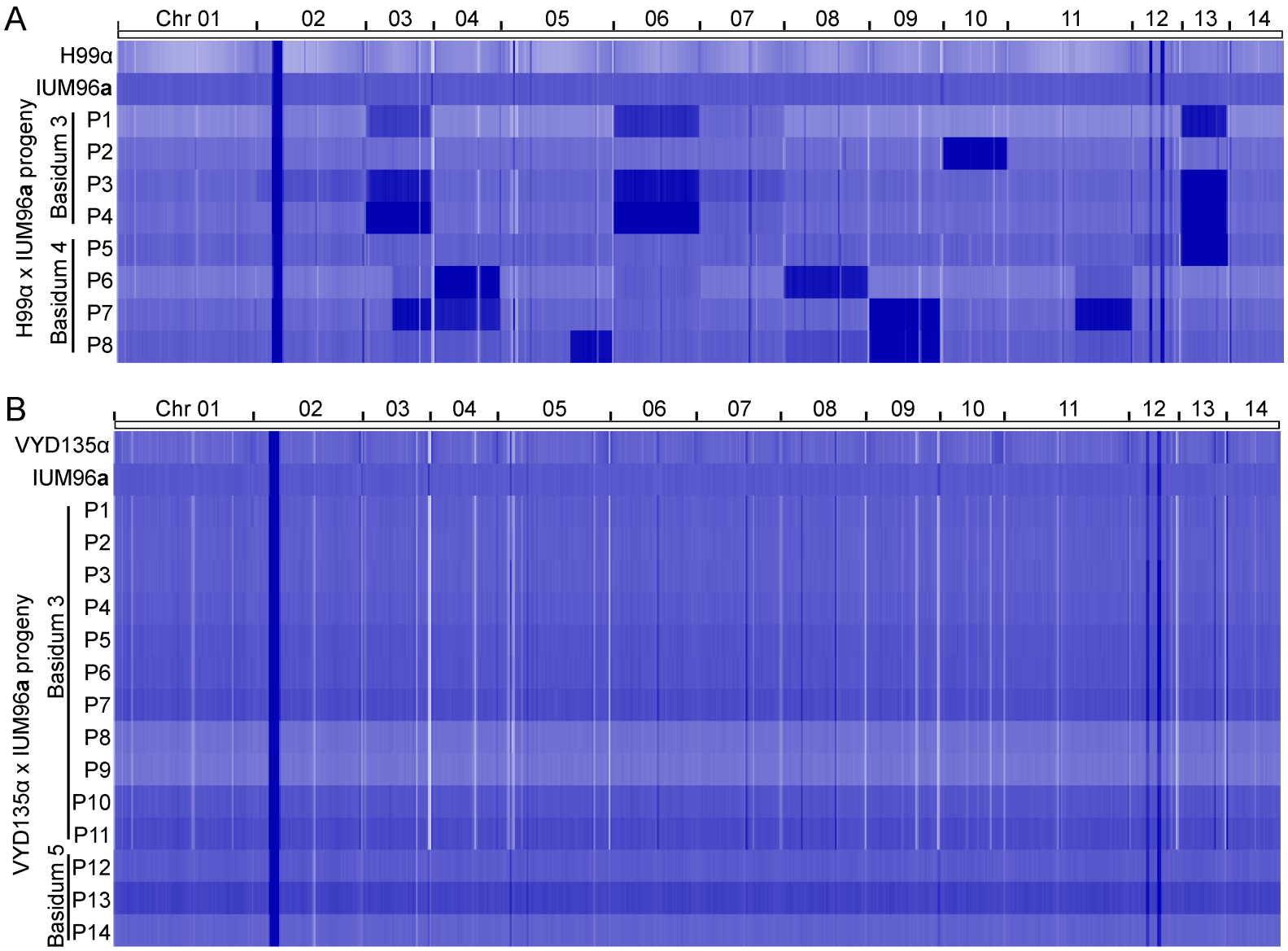
A
Chr 01
02
03
04
05
06
07
08
09
10
11
12
13
14
H99α
IUM96a
H99α x IUM96a progeny
Basidum 3
P1
P2
P3
P4
Basidum 4
P5
P6
P7
P8
B
Chr 01
02
03
04
05
06
07
08
09
10
11
12
13
14
VYD135α
IUM96a
VYD135α x IUM96a progeny
Basidum 3
P1
P2
P3
P4
P5
P6
P7
P8
P9
P10
P11
Basidum 5
P12
P13
P14

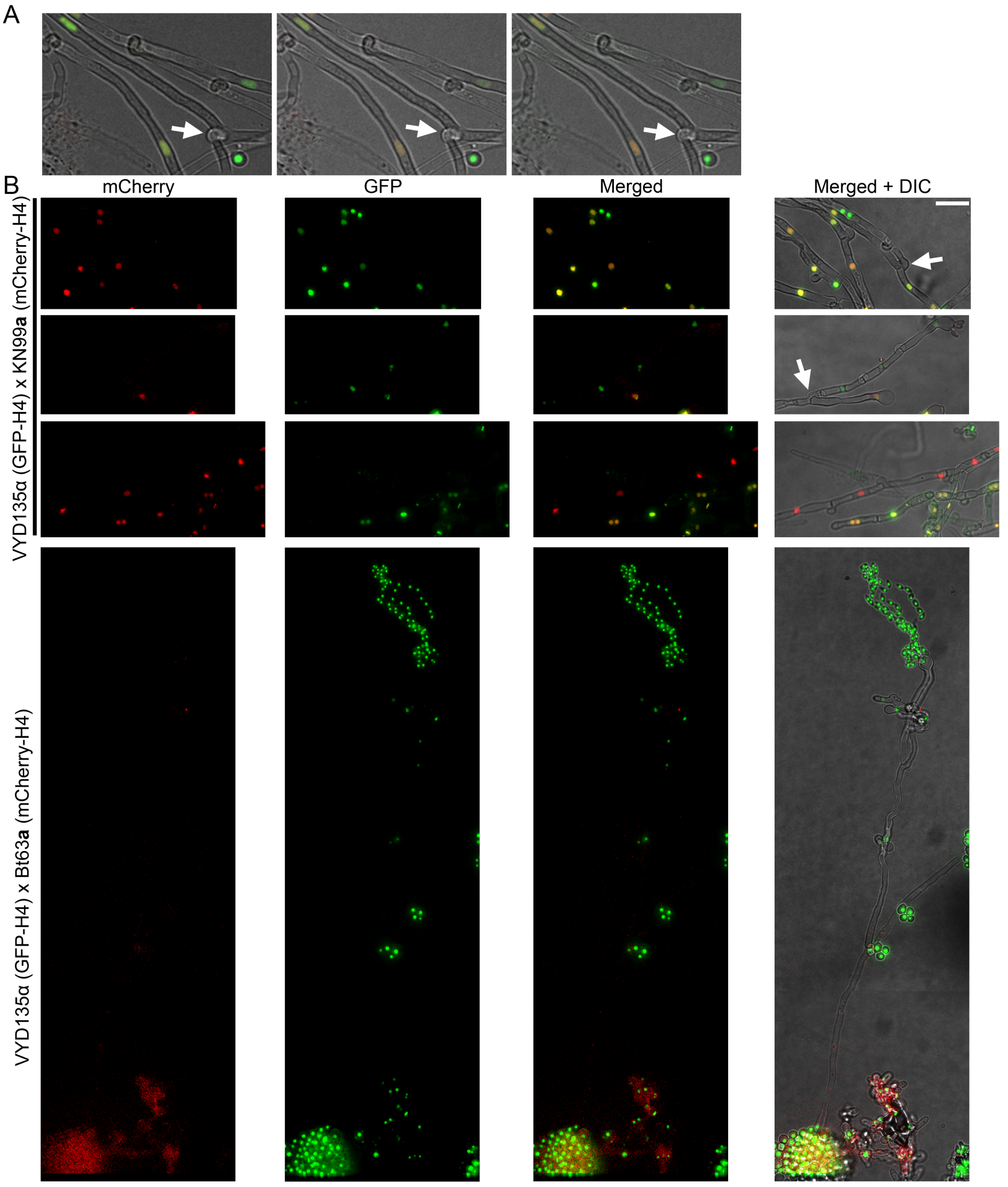
A
B
mCherry
GFP
Merged
Merged + DIC
VYD135α (GFP-H4) x KN99**a** (mCherry-H4)
VYD135α (GFP-H4) x Bt63**a** (mCherry-H4)

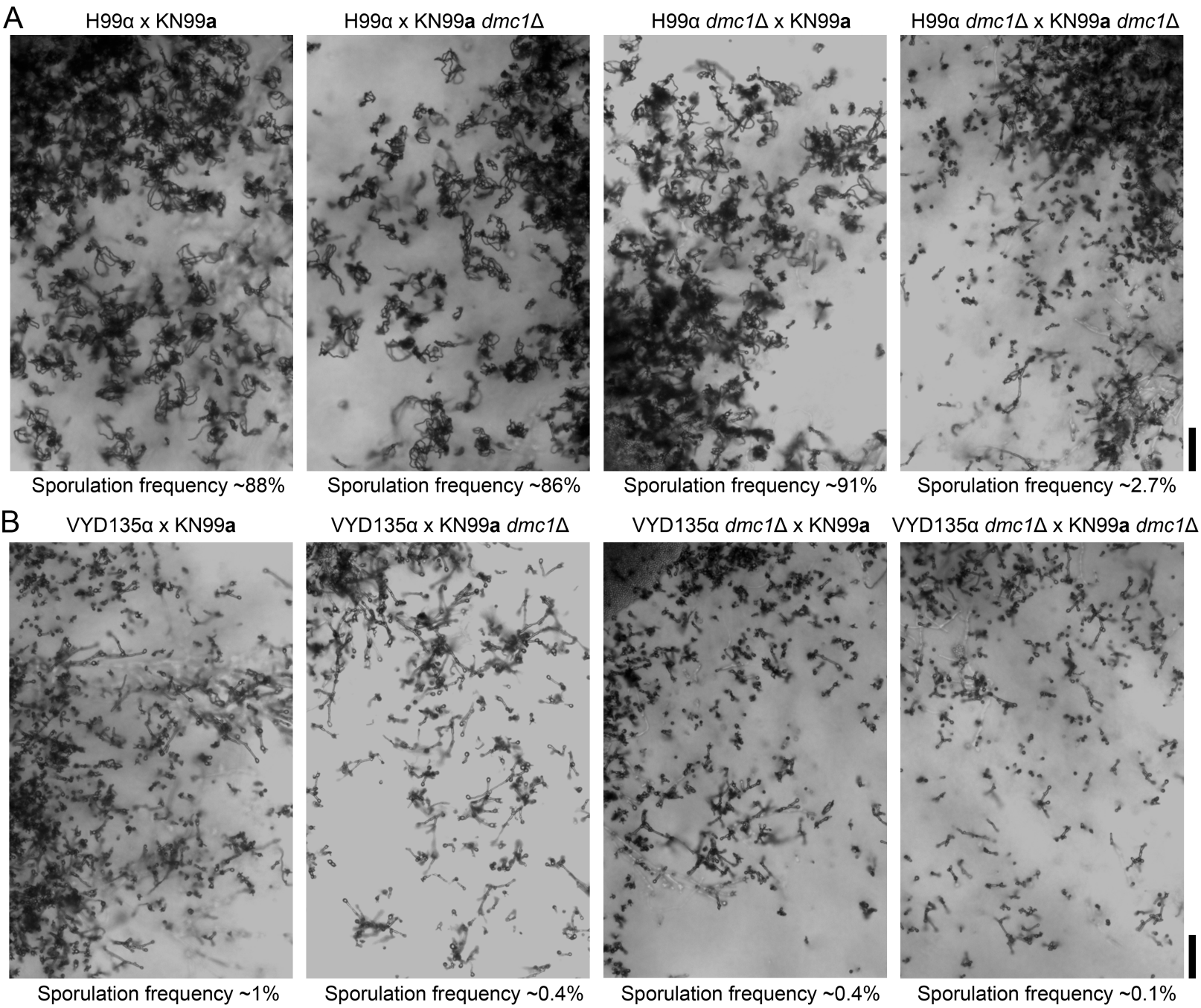
A
H99α x KN99**a**
H99α x KN99**a** *dmc1*Δ
H99α *dmc1*Δ x KN99**a**
H99α *dmc1*Δ x KN99**a** *dmc1*Δ
Sporulation frequency ~88%
Sporulation frequency ~86%
Sporulation frequency ~91%
Sporulation frequency ~2.7%
B
VYD135α x KN99**a**
VYD135α x KN99**a** *dmc1*Δ
VYD135α *dmc1*Δ x KN99**a**
VYD135α *dmc1*Δ x KN99**a** *dmc1*Δ
Sporulation frequency ~1%
Sporulation frequency ~0.4%
Sporulation frequency ~0.4%
Sporulation frequency ~0.1%

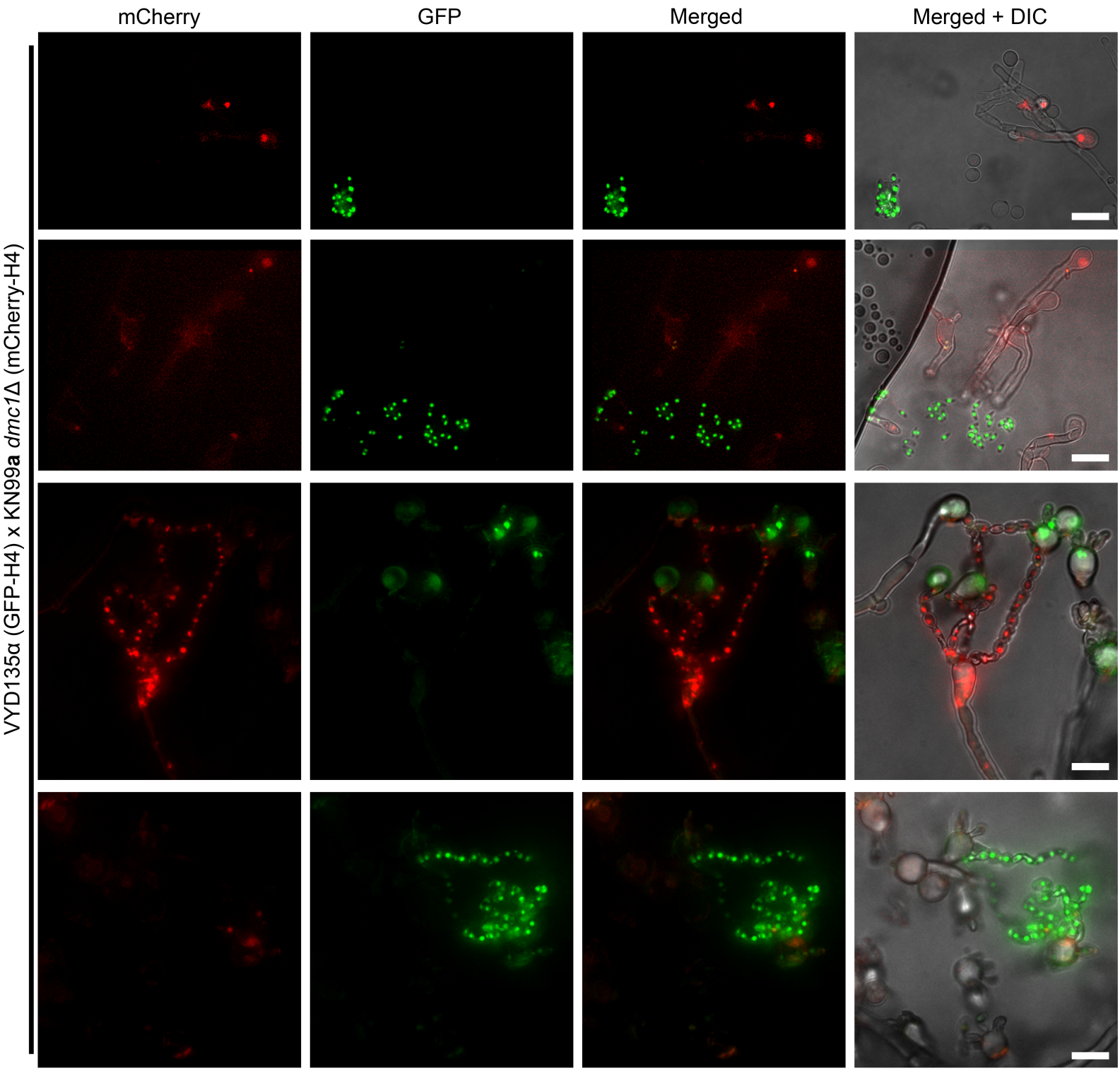
mCherry
GFP
Merged
Merged + DIC
VYD135α (GFP-H4) x KN99a dmc1Δ (mCherry-H4)

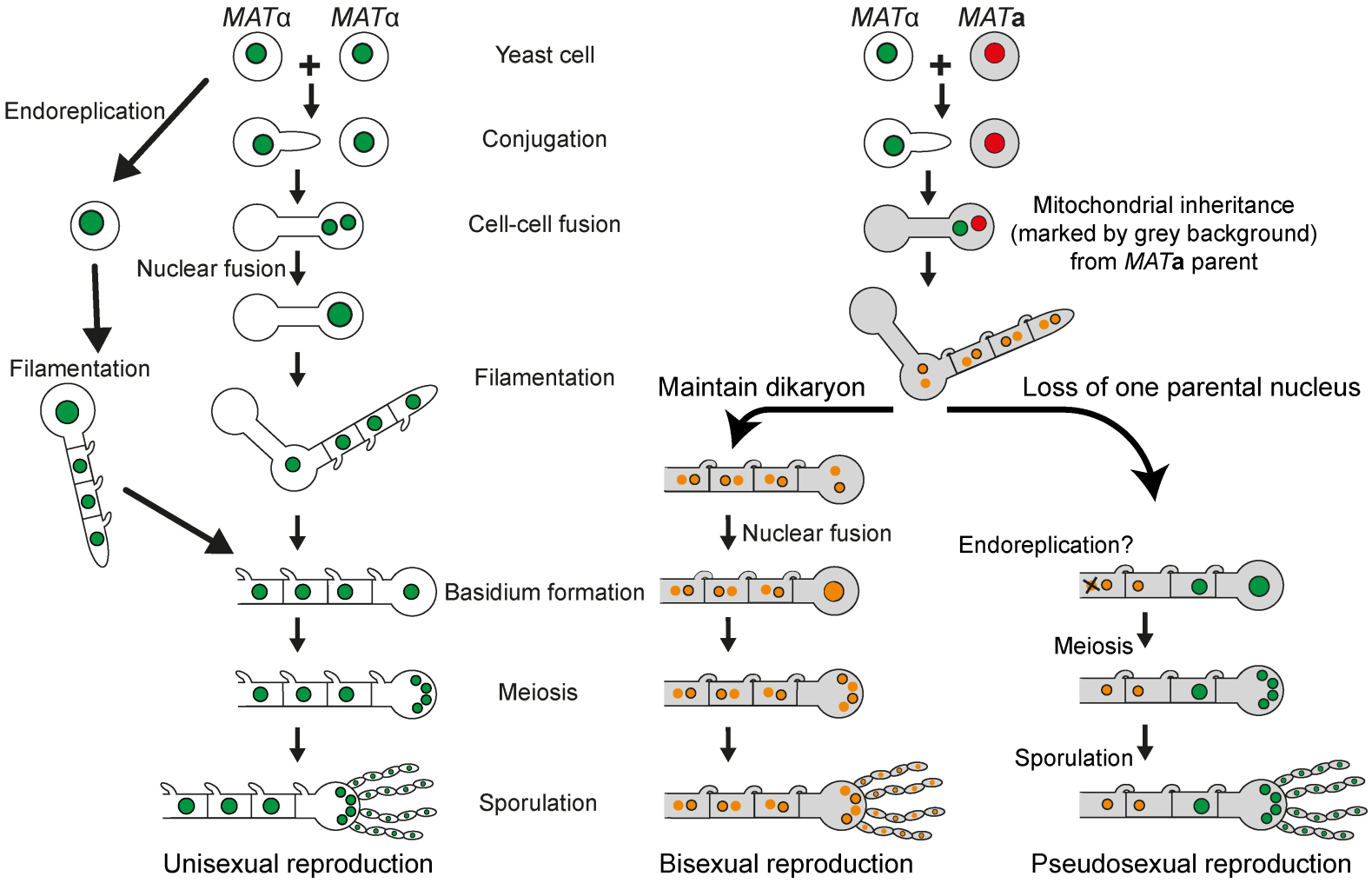
MATα
MATα
MATα
MATa
Yeast cell
Endoreplication
Conjugation
Cell-cell fusion
Mitochondrial inheritance
(marked by grey background)
from MATa parent
Nuclear fusion
Filamentation
Filamentation
Maintain dikaryon
Loss of one parental nucleus
Nuclear fusion
Endoreplication?
Basidium formation
Meiosis
Meiosis
Sporulation
Sporulation
Unisexual reproduction
Bisexual reproduction
Pseudosexual reproduction